A WIDEBAND RF APPLICATION OF FIBER OPTICS

Jessie Clarence Ross

NPS-32JR-74061

NAVAL POSTGRADUATE SCHOOL

Monterey, California

A WIDEBAND RF APPLICATION
OF FIBER OPTICS

Jessie Clarence Ross, Jr.
June 1974

Thesis Advisor: S. Jauregui, Jr.

Approved for public release: distribution unlimited.

Prepared for:
Naval Electronics System Command
PME-107
Washington, D.C. 20360

NAVAL POSTGRADUATE SCHOOL
Monterey, California

Rear Admiral Mason Freeman
Superintendent

Jack R. Borsting
Provost

This thesis prepared in conjunction with research supported in part by Naval Electronics Systems Command (PME-107), Washington, D. C. 20360 under P. O. 4-4579.

Released as a
Technical Report by:

UNCLASSIFIED
SECURITY CLASSIFICATION OF THIS PAGE (When Data Entered)

REPORT DOCUMENTATION PAGE		READ INSTRUCTIONS BEFORE COMPLETING FORM
1. REPORT NUMBER NPS-32JR74061	2. GOVT ACCESSION NO.	3. RECIPIENT'S CATALOG NUMBER
4. TITLE (and Subtitle) A WIDEBAND RF APPLICATION OF FIBER OPTICS		5. TYPE OF REPORT & PERIOD COVERED Thesis: July 73 - June 74
		6. PERFORMING ORG. REPORT NUMBER
7. AUTHOR(s) Jessie Clarence Ross, Jr. in conjunction with Stephen Jauregui		8. CONTRACT OR GRANT NUMBER(s)
9. PERFORMING ORGANIZATION NAME AND ADDRESS Naval Postgraduate School Monterey, California 93940		10. PROGRAM ELEMENT, PROJECT, TASK AREA & WORK UNIT NUMBERS P.O. 4-4579
11. CONTROLLING OFFICE NAME AND ADDRESS Naval Electronics Systems Command (PME-107) Washington, D. C. 20360		12. REPORT DATE June 1974 13. NUMBER OF PAGES 73
14. MONITORING AGENCY NAME & ADDRESS(if different from Controlling Office)		15. SECURITY CLASS. (of this report) Unclassified 15a. DECLASSIFICATION/DOWNGRADING SCHEDULE

16. DISTRIBUTION STATEMENT (of this Report)

Approved for public release; distribution unlimited

17. DISTRIBUTION STATEMENT (of the abstract entered in Block 20, if different from Report)

18. SUPPLEMENTARY NOTES

19. KEY WORDS (Continue on reverse side if necessary and identify by block number)

Fiber Optics
Light Emitting Diode
Photodiode
Analog Intensity Modulation

20. ABSTRACT (Continue on reverse side if necessary and identify by block number)

Recent progress in optoelectronic technology makes practical point-to-point optical data transmission systems consistent with military requirements and potentially far superior to wire techniques. This project provides a survey of the current state-of-the-art technology and investigates the feasibility of a fiber optic interface between a receiving antenna and radio receiver in the high frequency spectrum. An optoelectronic interface based on the use of conventional multimode fiber optics with a light emitting diode

DD FORM 1 JAN 73 1473 EDITION OF 1 NOV 65 IS OBSOLETE
S/N 0102-014-6601 |
(Page 1)

UNCLASSIFIED
SECURITY CLASSIFICATION OF THIS PAGE (When Data Entered)

20. continued

optical source and a hybrid silicon photodiode-preamplifier photodetector was designed, constructed, and tested. Signal reception for the interfaced system was observed throughout the receiver spectrum.

A WIDEBAND RF APPLICATION OF FIBER OPTICS

by

Jessie Clarence Ross, Jr.
Lieutenant junior grade, United States Navy
B. S., Berry College, 1969

Submitted in partial fulfillment of the
requirements for the degree of

MASTER OF SCIENCE IN ELECTRICAL ENGINEERING

from the

NAVAL POSTGRADUATE SCHOOL

ABSTRACT

Recent progress in optoelectronic technology makes practical point-to-point optical data transmission systems consistent with military requirements and potentially far superior to wire techniques. This project provides a survey of the current state-of-the-art technology and investigates the feasibility of a fiber optic interface between a receiving antenna and radio receiver in the high freguency spectrum. An optoelectronic interface based on the use of conventional multimode fiber optics with a light emitting diode optical source and a hybrid silicon photodiode-preamplifier photodetector was designed, constructed, and tested. Signal reception for the interfaced system was observed throughout the receiver spectrum.

TABLE OF CONTENTS

LIST OF ILLUSTRATIONS

LIST OF TABLES

I. INTRODUCTION

Recent advances in solid state optical sources and detectors and the fabrication of low loss optical fibers make their use practical in future communication systems. A fiber optic transmission system is considered potentially far superior to and offers inherent advantages over conventional electrical lines. The fact that fiber optics can reduce the size and weight necessary for a given bandwidth make it attractive for avionic applications. It also eliminates electromagnetic crosstalk and interference plus providing increased security since there are no radio frequency emissions and inductive coupling is impossible. Interface problems are decreased since the fibers provide total isolation between source and detector, thus eliminating ground loops, ground shifts in data circuits, short circuits, high voltage isolation, and ringing problems. The most promising advantage is the fact that as new processes become available and implemented we may in fact achieve the predicted ultra-broadband (1-10 GHz) bandwidth. Finally optical fibers offer potential economy.

The objective of this project was to determine the feasibility of a fiber optic interface between a receiving antenna and radio receiver in the high frequency (2-32 MHz) spectrum. The advantages cited above would alleviate many problems presently encountered onboard ships and aircraft. Many applications for such a system exist, notably where many sensors are co-located and data transfer from the sensor to a remote detector is necessary. This is the case in many shipboard situations and particularly so onboard submarines. This project was a preliminary attempt to apply the emerging optoelectronic technology to this problem.

II. BACKGROUND

A typical fiber optical transmission system consists of three basic components; the transmitter, the channel, and the receiver. Fundamental to each are the optical source, the optical fiber, and the photodetector respectively.

A. OPTICAL SOURCES

Various types of light sources are available. In general to ensure compatability, the light source used in an optical fiber system should meet the following requirements:

a. No special cooling required
b. Small, lightweight, and preferably inexpensive
c. Easily modulated
d. Fast response
e. Capable of continuous operation or high duty cycle
f. High radiant intensity
g. Small power consumption
h. Easily coupled to fiber.

Traditional sources such as incandescent, fluorescent, and gas discharge bulbs do not provide the necessary fast response in addition to being large in area, inefficient, and fragile. However, injection lasers, light-emitting-diodes (LEDs), and diode pumped neodymium-doped yttrium-aluminum-garnet (Nd:YAG) lasers satisfy most of the above requirements and are compatible with fibers. For the purposes of this discussion, the difference between the laser and the LED sources is that the laser possesses a substantial degree of temporal and spatial coherence while the LED does not. The effect of this incoherence is to limit LED compatability to multimode fibers.

1. Incoherent sources

Classical thermal and gas discharge sources are inherently inferior for fiber optic applications for a number of reasons. Though they produce watts of optical power they do so inefficiently, in a large spectral range, and even a large area. Additionally, they are fragile and subject to degradation and failure. Presently, the only suitable incoherent light source compatable with fiber optics is the LED which is small, cheap, rugged, reliable, efficient, and easy to modulate.

The LED [Ref. 1] emits light through the mechanism of electron-hole recombination in the PN junction region. Excess carriers are generated in the diode in the same manner in which minority carriers are injected into the base region of a bipolar transistor. For a zero-biased PN junction an inherent potential barrier prevents the large concentration of mobile conduction band electrons in the n-region from diffusing into the p-region. Similarly, the holes in the valence band are prevented from diffusing from the p-region to the n-region. Under forward bias the magnitude of the potential barrier is reduced, allowing diffusion of conduction band electrons and valence band holes across the junction. Once across, they significantly increase the minority carrier concentrations and these excess carriers then recombine with the oppositely charged majority carriers. This action tends to return the minority carrier concentrations in each region to their equilibrium values. The recombination of the excess minority carriers within a diffusion length L of the junction is the mechanism by which optical radiation is generated. The wavelength of the emitted light is a function of the material energy gap (E_G) between the valence and conduction bands and is given by

$$\lambda = \frac{1.24}{E_G}$$

where the energy gap is expressed in electron volts and the wavelength in microns. Pure GaAs with a gap of 1.4 eV emits in the near infrared region while other materials with larger energy gaps emit in the visible spectrum.

A performance limiting factor in LEDs is heat dissipation. The ninety percent of the electrical energy not converted to optical energy manifests itself as thermal energy and heats the material. The corresponding rise in junction temperature reduces the available output power in a non-linear fashion. The continuous wave (cw) output power is a linear function of input electrical power or drive current at low power levels, indicating that temperature effects are negligible. However, all LEDs display a saturation characteristic whereby above a certain current level a large increase in input current results in only a small increase in radiant intensity. This is due to an increase in relative nonradiative recombination probability as well as an increase in reabsorption of the emitted radiation. If the device is operated in the linear region with lower power levels, reliability is excellent.

The primary radiation pattern of the LED is Lambertian, i.e. the source radiates over an angle of 2π steradians. As a consequence, the actual radiation pattern of the device is determined, in general, by the internal geometry of the chip and the type of package used. The semiconductor chip containing the PN junction is normally mounted on a header and encapsulated. Most commercially available LEDs are silicon-doped solution-grown GaAs junctions with refractive optics for beam collimation. While these devices are characterized by high efficiency, their response times are relatively slow.

Planar diffused LEDs with good high speed characteristics are also available. Typically, the PN junctions of these devices are formed by zinc diffusion into n-type GaAs and have typical rise times of a few tens of nanoseconds. Several different device geometries are

available. The most basic is the flat geometry device in which the chip is header mounted and encapsulated beneath a transparent window. However, several physical phenomena limits the light output of the device to only a few percent of the total light generated. Basic to this is the fact that the refractive index of GaAs is so high, approximately 3.5 at standard emission wavelengths, that photons arriving at the chip surface-air interface with an angle of incidence greater than 15° are subject to total internal reflection and reabsorbed within the material.

This problem can be alleviated by the placement of a higher refractive index material on the chip. These are called shaped LEDs. Traditionally a hemispherical dome of epoxy has been used. However, truncated spherical emitters are now being considered for increased beam collimation and hence improved fiber optic coupling performance.

Diffused junction LEDs are also available as edge emitters. As the name implies the light is emitted from the edges of the chip and normally collimated through a contoured reflector package. This device overcomes the absorbtion problems encountered in other geometries. Proper design of the reflector allows focusing to achieve a narrow output beam. Refinement of the edge contour-reflector combination of the edge emitters is presently being considered for optimum coupling to the different numerical aperture fibers.

Manufacturers typically supply spatial radiation patterns. However, the fiber optic designer must realize these are normally far field patterns. As an example, location of an edge emitter within the reflector assembly causes the near field radiation pattern to be "donut" shaped. Far field patterns are cosine-law radiation patterns. These could more aptly be termed the diffuse source and point source patterns. This subtle fact can be important for close proximity fiber coupling.

LEDs are noted for fast response times. Neglecting

the electrical capacitance of the device, the limiting bandwidth factor is the carrier lifetime of the material which determines the fall time of the device. Carrier lifetime in typical commercial devices allow modulation frequencies of 30-100 MHz. Cut-off frequencies for the better developmental devices are approximately 150 MHz. This would limit the application of LED sources to direct use up to VHF signals and require baseband conversion of higher frequency signals.

2. Coherent sources

Since the first reported laser in 1960 numerous other lasers have been developed and demonstrated. Because of the primary concern here with fiber optics systems, let us begin with a specification of a laser suitable for communications through a fiber and then consider only those that agree relatively well within the boundaries specified.

Due to the effect of stimulated Raman and Brillouin scattering on the power handling capacity of low-loss optical fibers [Ref. 2], we would need a laser that produces more than a few milliwatts but no more than a few watts of monochromatic continuous power. It should have excellent frequency stability and be tuneable to any of a large number of frequencies in the visible and into the near infrared (IR) region of the spectrum. It should be relatively efficient with the light output being at least a few percent of the electrical power input. It should operate at room temperature and not require special cooling or elaborate heat sinks. It should operate in a single mode, preferably the fundamental mode of the fiber. Furthermore, it should be compact and easily handled, have a long lifetime, and not require a high voltage power supply for operation.

Gas lasers, such as the HeNe, Ar ion, and CO lasers, are numerous and available. However, they are not candidates for fiber systems for a number of reasons. For instance, because of the CO emission at 10.6 microns, it is

not of interest due to the intrinsically low transmission of fibers this far in the infrared. Though gas lasers are difficult to discuss as a group because of the diverse properties they possess, one might attempt a rough generalization from a fiber system compatability perspective by saying that, in general, gas lasers have too low an efficiency, too short a life, a large power requirement, do not offer any of the tuneability necessary for the provision of adequate numbers of carriers for frequency multiplexing, plus cost and size disadvantages when compared to semiconductor devices.

The laser most nearly meeting all the aforementioned specifications is the semiconductor injection laser. Recombination of injected electrons with holes in a forward biased PN junction region is the radiation mechanism in this device, just as in an LED. However, the design of the two devices is considerably different. The injection laser has the edges of the chip polished to create a cavity parallel to the plane of the chip which forms a Fabry-Perot resonator. Due to the very high population inversion, when the current density (threshold) is sufficient to increase the stimulated emission gain of the diode above the cavity attenuation, the diode lases. The intense light is emitted from the approximately two micron wide junction with a wavelength approximately equal to the wavelength of the spontaneous emission. Although special structures can be devised to minimize the emerging beam's divergence, this laser suffers from more dispersion than other laser types. Typical beam divergences are 5° parallel to the junction plane and 15° perpendicular to it. The most advanced of the injection lasers are those made of GaAs but many other less efficient materials have been investigated. An immediate disadvantage with semiconductor lasers is the fact that the power levels achievable depend on the operating conditions. At liquid nitrogen temperatures, several watts of CW coherent radiation can be obtained. But at room

temperature, because of internal power dissipation (absorption and nonradiative recombination in the medium) the laser is limited to pulsed operation. Typical commercial devices at room temperature have a duty cycle of 0.1%, a maximum pulse repetition frequency of 50KHz, and questionable reliability. Recent work to alleviate this limitation has focused in broad area junctions where the injected electrons are confined to a region very near the junction (the resonator region) by putting a thin layer of GaAlAs on both sides of the laser (a so called heterojunction) and relying on the higher energy band-gap for confinement. This progress has reduced the critical parameter threshold current low enough to allow room temperature operation. Continuous operation in a laboratory has been demonstrated at room temperature of stripe-geometry double heterostructure uncoated Fabry-Perot junction lasers at wavelengths from .773 to .9 micron. However, the one remaining obstacle of device life has yet to be completely overcome. Progress has been made in isolating the causes of degradation of these devices.

In general, semiconductor lasers offer us high efficiency (up to 10 %), output power of the order of tens of milliwatts, small size, no requirement for a high voltage supply, and a range of wavelengths by varying the chemical composition. Plus the injection laser can be easily amplitude modulated by direct electrical modulation of the current through the junction. Since the laser diode is relatively new, further improvements in the devices should make them highly amenable to wideband single mode fiber optics systems of the future.

Of the solid-state ion lasers, the most promising is the Nd:YAG when pumped by efficient incoherent electroluminescent diodes. A serious limiting feature for many applications is the flowing water cooling requirement. However, recent advances indicate conductively cooled operation may be a feasible alternative. The dimensions of

this laser make it suitable for easy coupling to fiber optics. However, an external means of modulation must be provided. For the design engineer, the external modulator requires additional real estate and represents an additional cost factor.

Another area currently under investigation is a fiber laser which is based on the fact that a fiber can serve as the cavity resonator required for laser action. It is expected that fiber lasers may have lower operating thresholds than present lasers and consequently require less input power. Although not yet realized, it is indeed an intriguing possibility.

Practical engineering considerations strongly favor the semiconductor injection laser. Metallurgical improvements of the long term operating life of these devices under continuous operation at room temperature are a must. Future very wideband single mode fiber optics systems will undoubtedly use a reliable CW semiconductor injection laser.

B. OPTICAL FIBERS

The bandwidth potential of optical communications has been recognized for some time but the non-availability of a suitable low-loss transmission medium has inhibited realization of that potential. However, a 1970 report of attaining losses in the order of 100-200 dB/km in short lengths of fibers provided the first true indication that optical communications over fibers for extended distances might be realizable. More recently, in mid-1972 an attenuation of 4 dB/km was achieved at wavelengths of 850 and 1060 nanometer; with all losses between 600 and 900 nanometer below 12 dB/km [Ref. 3]. Current experiments indicate the ultimate lower limit is about 2 dB/km [Ref. 4]. These levels will make possible communications over distances of a few kilometers without repeaters.

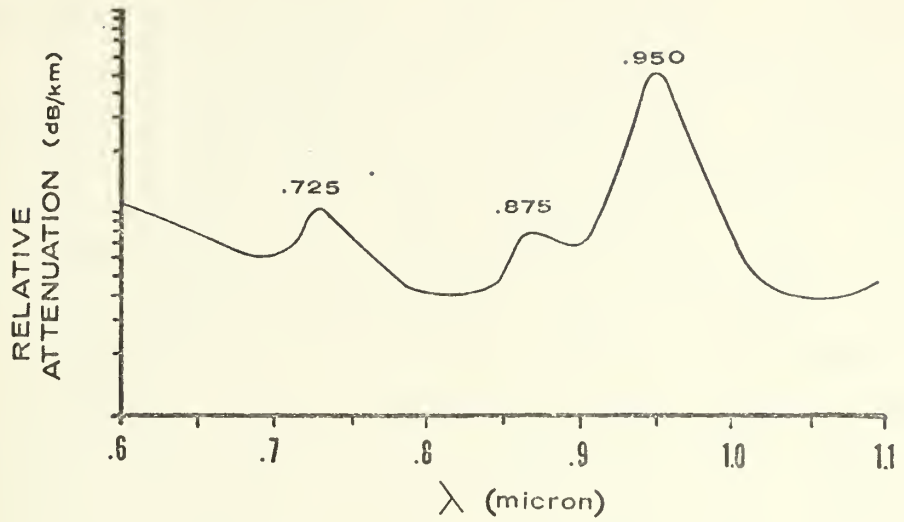

FIGURE 1 FIBER OPTICS SPECTRAL ATTENUATION

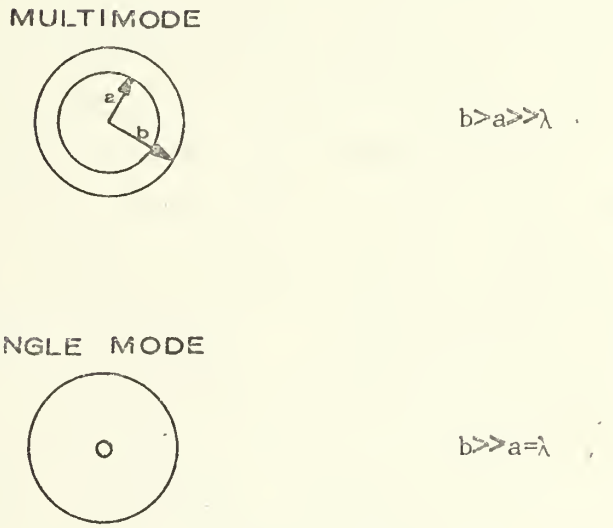

FIGURE 2 STEP REFRACTIVE INDEX FIBER GEOMETRY

Figure 1 typifies the relative spectral attenuation characteristics of most of the waveguides manufactured to date in both the multimode and single configuration. The sources of attenuation in fibers are absorption, or conversion of light into heat due to nonuniformities in the refractive index of the material, and scattering. Furthermore, absorption consists of three types: intrinsic, impurity, and atomic "defect" color centers. Scattering also consists of three types: intrinsic, glass inhomogeneity, and aberrations in the radial or cross-sectional form of the refractive index [Ref. 5]. Let us use the spectral attenuation curve to examine these attenuation effects. For the region below .6 micron, the most important contribution is the attenuation coefficient of intrinsic material absorbtion. In the region .6-1.6 micron the mechanism of interest is the "water" impurity or hydroxyl ion (OH) absorption. This contributes the easily identifiable attenuation peaks around .95 and .725 micron. These are, respectively, the third and fourth harmonics of the 2.73 micron fundamental vibration of the OH radical. Other absorption bands including the .875 micron band, have been determined to be combinations of the various OH harmonics and harmonics of the fiber material fundamental vibration. Achieving 2 dB/km would require a marked reduction of the fibers OH content leaving scattering as the major loss mechanism. Attenuation due to impurity absorption arising from transition-metal ions such as iron, cobalt, and chromium is the dominant loss mechanism in commercially available medium-loss or conventional fibers. A loss of 20 dB/km requires impurity concentrations below a few parts per billion. Thus the primary problem is that of achieving glass purification during the fabrication process.

In view of the scattering loss due to induced aberrations in the refractive index, an important application consideration is the minimum bending radius allowable for the fibers. Mechanically the minimum bend

radius of a fiber is limited by the fibers stiffness and is a function of its diameter. Radii of curvature of several centimeters are tolerable for all types of fibers. Consequently, bending losses will, in general, be of negligible importance in realistic application configurations.

Several fabrication techniques are commonly used to draw fibers. Three main methods are: double-crucible, rod-in-tube, and ion exchange [Ref. 6]. The double-crucible technique employs two concentric crucibles with the inner crucible containing the higher-index core glass and the outer crucible containing the lower-index cladding glass. The contents of both crucibles are heated to melting and the fibers are drawn. This technique has been successfully used in the drawing of both single-mode and multimode fibers.

A second technique is the rod-in-tube or preform method where a rod of higher-index core material is inserted in a hollow cylinder of lower-index material. The nozzle end of the rod and cylinder are heated to soften the materials and the fiber is drawn from the necked down section at a constant rate. Again both single mode and multimode fibers can be fabricated by this method.

A third technique is ion exchange. A glass fiber rod of homogeneous glass is immersed in a hot salt bath. The monovalent alkali ions of the salt and ions in the glass interchange in a controlled diffusion process. By stopping this process before complete ionic exchange occurs, a parabolic index profile is obtained. After the ion-exchange period, the glass rod is heat stretched to make long fibers. The primary limitation of this method is the fact that fibers produced are of limited length, typically less than 20 meters. However, recently the Nippon Sheet Glass Company has developed a new continuous manufacturing process using fast ion exchange in a special double-crucible method [Ref. 7]. The inner and outer crucible conain borosilicate glass with TI ions (refractive index 1.542) and Na ions

(refractive index 1.489) respectively. The ion exchange takes place in the vicinity of the nozzles of the crucibles because of high temperature, with the net result of no distinct boundary between the core and cladding. Typical fiber drawing speed is a few tens of meters per minute. The principles of this light-focusing fiber, tradename SELFOC, will be discussed in more detail later.

A few basic principles and definitions of waveguide pheromena are necessary to clarify the aforenemtioned manufacturing methods. The foundation of fiber optics is the principle of total internal reflection. In optical fibers this is accomplished through a refraction effect on the light rays propagating in the fiber. Two basic methods exist to confine the light in the fiber. One method is the step-refractive index where the fiber has a core clad with a material of a lower refractive index. Another method is the graded index (GRIN) guide in which the fiber has a high refractive index on its longitudinal axis which decreases approximately as the square of the radial distance until the surface is reached. In addition to these confinement techniques, there are basically two classes of fibers: those that propagate only one mode of radiation (single mode) and those that propagate many modes (multimode). Figure 2 shows both pictorially. Extending the microwave hollow metallic waveguide to optical frequencies is impractical because of a high sensitivity to bends.

A light beam propagating in a cylindrical fiber core of high index material surrounded by a cladding of lower index will be confined by total internal reflection if

$$\sin \theta \leq \sqrt{n_1^2 - n_2^2}$$

where n_1 and n_2 are the refractive indices of the core and cladding respectively and θ is the angle between the propagation vector of the incident beam and the axis of the fiber cylinder. Additionally, each internally propagting ray must strike the core-cladding interface with an angle of

incidence greater than the Snell's Law critical angle without exception as it traverses the length of the fiber. Cladding thickness is usually several wavelengths to ensure all modes coupled in the fiber propagate within the core and cladding. Overall diameters of fibers manufactured have been from several microns to several hundred microns.

An important parameter for circular or cylindrical fibers with step-refractive index variation is

$$V = \frac{2\sqrt{2}\,\pi r}{\lambda} \quad (\bar{n}\Delta n)^{\frac{1}{2}}$$

where r is the core radius, λ is the free space wavelength, is the average refractive index of core and cladding, and n the difference in refractive indices between core and cladding [Ref. 5]. For values of V below approximately 2.4 the fibers propagate only the lowest order mode (of a hybrid character) and one has a single mode fiber. Above this value the number of propagating modes increases rapidly with the approximate number given by $V^2/2$. Furthermore, assuming all modes are equally excited, the approximate ratio of cladding power to total power is 8/3V.

The chief advantages of the single mode fiber are its low pulse distortion and large information-transfer bandwidth capability: 10^{11} bit/sec/km [Ref. 3]. Since it is not possible to combine large core area and large acceptance angle and the single mode propagation characteristic of the fiber itself, a laser source is required. Until a CW, room temperature solid state semiconductor is commercially available, this is a serious limitation. Also, the small entrance aperture can pose engineering problems in adequate source alignment.

The multimode fiber with the step-refractive index profile is commercially available and has been used in many recent applications because of its compatability with existing sources and detectors, notably the moderately priced LEDs and photodiodes. Since the incoherent light of

LEDs can not be injected into a single mode fiber with high efficiency, multimode fibers must be used. the multimode fiber can have both a large core area and large acceptance angle. However, the information-transfer bandwidth of the multimode fiber is approximately three orders of magnitude less than the single mode fiber; slightly above 10^8 bit/sec/km [Ref. 3].

Another class of multimode fibers are the graded-index (GRIN) or self-focusing (SELFOC) guides which are fabricated to have a radial index variation of the general form

$$n = n_o \operatorname{sech} \rho r$$

or by expanding and neglecting higher order terms

$$n = n_o \left(1 - d\,(r/a)^2 \right) \quad , \quad r > a$$

where n_o is the refractive index on the fiber axis, ρ the radial variation constant related to the focusing distance, r the radial distance from the fiber axis, a the distance from the axis where the refractive index is $n_o(1 - d)$, and d is the difference of the cladding and core refractive indices.

If the input light is injected at an angle with respect to the axis of a GRIN fiber it will oscillate about the axis with a period given by a wavelength (λ)

$$\lambda = \frac{\pi a}{n_o (2d)^{\frac{1}{2}}}$$

From a practical viewpoint, the primary advantage of these fibers is the fact that since all modes corresponding to meridional rays (HE_{1m} modes) have the same group velocity. Therefore, though many modes are excited, they should experience very little spread during transmission in the fiber. Transmission capacity for the new SELFOC fiber is larger than 10^9 bits/sec for one kilometer [Ref. 7] which is much more favorable than that of the more typical clad fiber

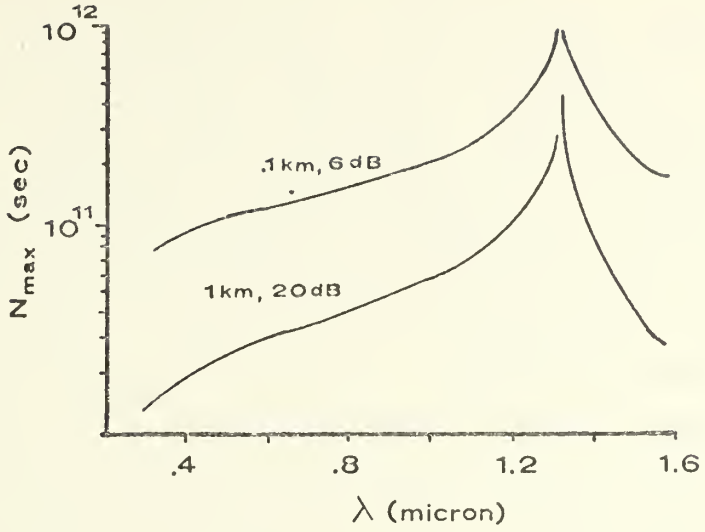

FIGURE 3 CALCULATED INFORMATION RATES FOR A TYPICAL SINGLE MODE FIBER WITH ADJACENT PULSE OVERLAP EXPRESSED IN dB

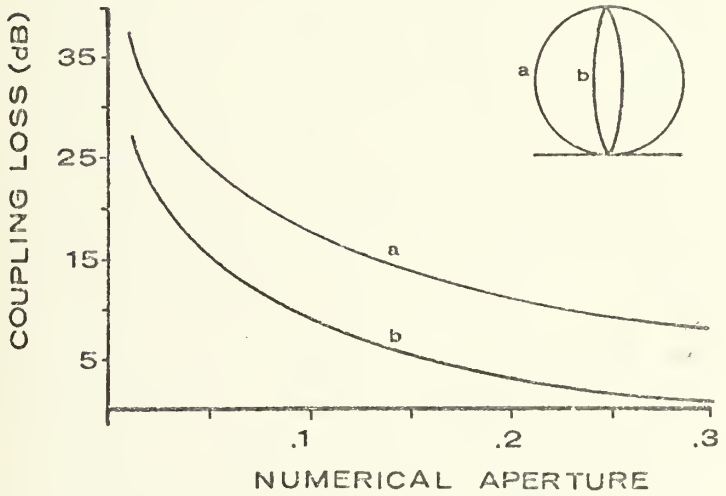

FIGURE 4 FIBER NUMERICAL APERTURE COUPLING LOSS FOR a) LAMBERTIAN AND b) 10^{o} BEAM HALF-ANGLE LED SOURCE

with step-refractive index profile.

Of prime importance for realistic applications is the information-carrying capacity of fibers. Many physical factors affect the allowable data transfer rate through fibers including birefringence, backscattering, and dispersion. Birefringence properties of fibers due to local variations in the elliptical core form and very small stress distributions result in a calculated information rate limited to 10^{12} bits/sec for low-loss single mode fibers [Ref. 8]. The backscattering effect due to multiple back and forth scattering introduces a delay with respect to the signal for the scattered light. Considering a pulse train, these delays essentially act as background interference. Analytically, it has been shown that backscattering will not be a serious problem in limiting bandwidth for typical fibers [Ref. 9]. However, at high power-densities backward-wave stimulated scattering processes (either Raman or Brillouin) will result in a severe attenuation of the signal due to the transfer of energy to the stimulated backward wave. Both the Raman and Brillouin scattering processes introduce power dependent losses when they become stimulated and, hence, impose limitations on the power handling capability of the optical fiber. For multimode sources stimulated Raman scattering will set the upper limit on the fibers power handling capability, while for single mode sources stimulated Brillouin scattering will dominate. The critical power due to the Brillouin effect is approximately two orders of magnitude less than that due to the Raman effect. the estimated critical power for a 20 dB/km single mode fused silica fiber with an area of 10^{-5} mm^2 is 35 mW for a CW single longitudinal mode laser [Ref. 2].

For single mode fibers the information-carrying capacity is determined by pulse broadening due to material and individual waveguide dispersions. Calculated information rates for a typical single-mode fiber are given in Figure 3

[Ref. 3]. At the singular point near 1.3 micron the glass or material dispersion cancels the waveguide dispersion and the bandpass becomes quite large. This is uniquely intriguing, but present needs can be met at any of the other wavelengths.

Multimode step-refractive waveguides are also characterized by these same dispersion mechanisms. However, multimode dispersion is also caused by the fact that the group velocity of the guided modes is not the same. The injected input power is shared by any or all of the possible modes and, as a consequence of the differing group velocities, will emerge at different times. Approximations of this modal dispersion phenomena are made using geometrical ray optics with the pulse width taken as the time between the straight-through ray and the ray at the critical angle which sustains multiple reflections in traversing the fiber. Currently the limit on information transfer capability of these fibers is 10^8 bit/sec/km. Current efforts to reduce the effects of the differing group velocities in these fibers involve a proviso for coupling between the guided modes [Ref. 10]. The GRIN fibers with parabolic index profile exhibit less pulse delay distortion since the group delay differences are nearly equalized. The pulse spread is approximately one order of magnitude smaller than that of a fiber with an equal, but abrupt, index decline from core to cladding [Ref. 11].

Various modified parabolic index profiles have been explored analytically to find the optimum profile to maximize the fiber performance characteristics. However it remains to be seen whether the necessary index gradient tolerances theory dictate can be achieved or maintained in a production facility.

Injection and extraction of light from the fiber or fiber bundle must also be considered. Launching of angularly distributed light from a spatially distributed source such as an LED will introduce losses due to Fresnel

reflections at the fiber end, the limited numerical aperture (NA) of the fiber, and the packing fraction (PF) of the bundle. The numerical aperture of a fiber is the acceptance half-angle, $\theta/2$. Descriptively, it represents the acceptance cone size or, equivalently, a measure of the flux accepting capacity of the fiber. Typical values for conventional and low-loss fibers are 0.6 and 0.14 respectively. Losses due to NA are essentially a collection loss and development of an LED with improved internal beam collimation will minimize this effect. Figure 4 illustrates this point. Fresnel reflections due to an index mismatch boundary can be minimized by minimizing the difference between refractive indices. Packing fraction is the ratio of active core area to the total bundle area and is made of two parts; the fraction of the circumscribed circular area of the bundle covered by the fibers and the fraction of each fiber covered by the core glass. Present bundles of hexagonal close-packed multimode fibers typically have a packing fraction of approximately 25% for low-loss fibers and 60% for conventional fibers.

The coupling problems associated with multiterminal communications using multimode fibers have prompted the development of four basic coupler designs: STAR, modular STAR, "T", and multiple "T". As the names imply there are two principle coupler types. The STAR coupler approach is primarily designed to overcome the low PF-NA effects of low-loss fibers. The "T" coupler is intended for use with conventional fibers and in one form uses a scrambler rod to ensure uniform distribution of energy to all fibers. Other forms of "T" couplers are in the developmental stage. Continuing work to optimize the design criteria of each coupler as a function of fiber bundle size, NA, and PF should result in the availability of an off-the-shelf family of access couplers in the near future.

There is one problem that can not be disregarded for military applications. In general, optical glass is

sensitive to nuclear and cosmic radiation which causes a browning or darkening of the glass that reduces its transparency. It has been estimated that fibers using a glass core susceptible to this phenomena would be limited to a useful life of ten years [Ref. 12]. Several facilities are presently studying the effects of radiation induced light generation, index modification, optical absorbtion, and light scattering. Progress has been made by the Naval Research Laboratories in radiation hardening by cerium doping of high purity silicate glasses for conventional fiber optics and very strong oxidizing conditions during fiber preparation for low-loss doped silica fibers [Ref. 13]. However, extensive testing of fast and thermal neutron radiation effects must be done to ensure fiber reliability onboard nuclear powered platforms.

While remarkable progress has been made in the fabrication of low-loss fibers for optical communications, further work remains in developing the practical techniques and hardware (i.e. optical couplers, splicers, connectors, bundling and jacketing techniques, plus electronic devices) needed to use fibers effectively and efficiently. Bundling is the grouping of many fibers together. Bundles are normally jacketed by a PVC or teflon type plastic as a protective coating against the environment and to enhance their handling characteristics. Cabling of one or more bundles will be necessary for practical field handling and installation. Cabling techniques are being investigated at several facilities. One current approach is a hexagonal array of six fiber bundles around a solid core support with a surrounding jacket. This cable is concentrically located inside an outer jacket and supported by two smaller cylindrical wires which provide the necessary tensile strength.

Interfacing with existing systems will require development of standard connectors. Modifications of BNC, multipin, and specially machined connectors are now being

used. However, no standardized interconnectors or field repair techniques have been adopted to date.

Uniform tests and test procedures must also be developed to characterize the physical properties of fiber optic bundles and cables. Both mechanical strength properties and environmental performance tests are needed to reflect the structural integrity and operability of fiber optics. A two year program at the U. S. Naval Electronics Laboratory Center has produced tests for bending radius, tensile strength, mandrel strength, twist, flexibility, vibration, mechanical shock, flammability, thermal, humidity, salt spray, and chemical effects [Ref. 14]. It preliminarily appears that fiber optics will be able to stand the rigors of shipboard and avionic operation.

A significant by-product of the development of low-loss fibers has been the tremendous boost in research efforts to develop integrated optics circuits (IOCs). Analogous to an electronic integrated circuit, the IOC will contain many optical components on a single substrate and should offer advantages in size, weight, power consumption, cost reduction with increased speed, reliability, and ruggedness. However, it is anticipated that they will not find application in communications until data rates exceed 300 Mb/sec and spatial multiplexing is extensively used [Ref. 15]. Functions they might provide include light generation, modulation, detection, switching, directional coupling, repeaters, spectral filtering, fan in and fan out, plus other signal processing functions. Multiterminal access to the same fiber is an important feature that might well be realized in wideband systems only through IOCs. It is expected that these miniature optical circuits will play a central role in the evolving fiber optics technology.

C. PHOTODETECTORS

As in the case of light sources, many photodetectors are

presently available. Within the bounds of fiber optics systems one may impose certain general requirements, namely:

a. Require no special cooling
b. Converts optical signal to electrical signal
c. Small power consumption
d. Fast response
e. High sensitivity
f. Peak response near transmitter wavelength
g. Small, lightweight, and preferably inexpensive
h. Easily coupled to fiber
i. Instantaneous bandwidth wider than signal bandwidth
j. Minimum noise addition to signal.

Photodetectors useful for optical communications are square law detectors whose output current is proportional to the square of the electric field in the optical wave averaged over the active area of the detector. Although this provides the possibility of mixing a phase or frequency modulated signal with a local oscillator to give heterodyne or homodyne detection, they compare unfavorably with direct detection in fiber systems where background radiation is avoided. In a direct detection system, where the carrier is intensity modulated and not mixed with a local oscillator, the general relation between the generated photocurrent and an incident light of power P and optical frequency ν is

$$I_s = N \frac{ePG}{h\nu}$$

where I_s is the signal current, N is the quantum efficiency of the detector, e is electronic charge, G is internal gain of the detector, and $h\nu$ is the photon energy.

Proper design of detection systems for optical communications is a must. The information bandwidth of the communication system determines the longest time constants that are permissable in the photodetector and associated output circuitry. Detector shunt capacitance, series resistance, and circuit parasitics have to be considered.

Thus the speed of response of the detector and the bandwidth of the receiver is a function of the receiver circuitry. The bandwidth of the receiver in terms of a load resistance, R, and shunt capacitance, C, is

$$B = \frac{1}{2\pi RC} \quad .$$

The signal-to-noise ratio and the minimum detectable signal are the ultimate criteria by which the receiver sensitivity is judged. The two principal types of noise added to the signal are shot noise and thermal noise. Shot, or Schottky, noise is due to statistical fluctuations in the rate at which current is generated by the detector. Thermal, or Johnson, noise is due to random fluctuations in the thermodynamic energy stored in the load resistor. The signal-to-noise ratio at the output of a generalized direct detection system using a photodetector with internal gain G is

$$\frac{S}{N} = \frac{I_s^2}{I_n^2} = \frac{I_s^2}{2e\,(I_s+I_d)\,GB + \frac{4kTB}{R}}$$

where I_d is the dark current that is multiplied with the photodetector, $\frac{4kTB}{R}$ is the effective mean-square thermal noise current, GB is the detector gain-bandwidth product, and T is the effective noise temperature.

Before discussing particular photodetector devices, their performance characteristics which are of importance in determining the overall optical communication system performance are:

a. Efficiency in the conversion of optical radiation to signal current

b. Time dispersion effects within the device which may limit bandwidth

c. Internal gain mechanisms which may be used to amplify the primary photocurrent

d. Internal noise sources which may limit system sensitivity.

The best semiconductor photodetector is the photodiode. The photodiode basically consists of a semiconductor in which the current or voltage is a function of the incident light which generates electron-hole pairs in or near the depletion layer of the PN junction. Photodiodes can be operated in the photovoltaic mode (zero bias voltage) where it can be considered a voltage source and in the photoconductive mode (reverse bias voltage) where it can be considered a current source. In the photoconductive mode the amplifier assumes the responsibility for current to voltage conversion with good frequency response and low noise level. The device working into a low impedance load operates at maximum bandwidth. In the photovoltaic mode, the signal current is converted to a voltage across a high valued load resistance with subsequent voltage amplification. These diodes are normally operated in the reverse bias region because the photoconductive mode yields a larger responsivity at wavelengths greater than 0.9 micron and a wider spectral bandwidth than the photovoltaic mode of operation. The ac characteristics of photodiodes can be described in terms of an equivalent circuit shown in Figure 5 that contains signal, noise, and dark current generators; diode junction capacitance and resistance; plus bulk series resistance. The diode junction resistance is very high, typically of the order of many megohms. The diode capacitance depends on the applied voltage V and the active area A by the relation

$$C = \frac{2 \times 10^4 \, A}{\sqrt{pV}} \quad pF.$$

where p is the resistivity of the material in ohm-cm [Ref. 16].

The quantum efficiency for a particular photodiode depends on the incident light wavelength and the depletion layer width. For incident wavelengths with energy near the energy gap of the diode material, light penetrates deeply within the material. Consequently, high quantum efficiency

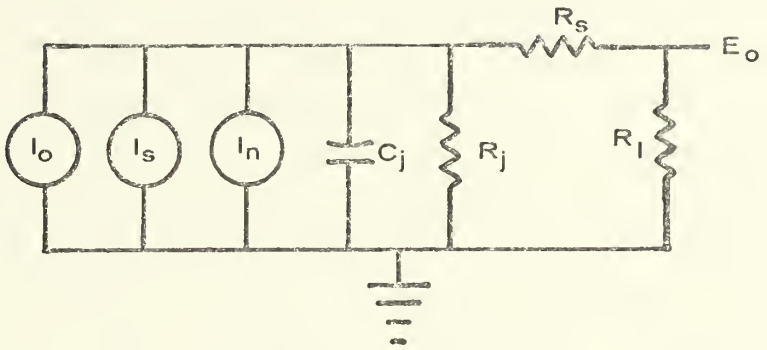

I_o ___ dark current

I_s ___ signal current

I_n ___ noise current

C_j ___ junction capacitance

R_j ___ junction resistance

R_s ___ bulk series resistance

R_l ___ equivalent load resistance

FIGURE 5 PHOTODIODE EQUIVALENT CIRCUIT

requires wide space charge layers which leads to relatively long carrier transit times. In the visible and near infrared, photodiodes with high quantum efficiency, fast speed of response and low dark currents are available.

The best devices are a modification of the basic PN junction structure with a relatively wide intrinsic layer separating the heavily doped P and N regions (the "PIN" structure). The depletion region extends throughout the intrinsic layer resulting in an increase of the effective thickness of the active region. Control of the intrinsic layer width allows an adjustment of the effective depletion width. Thus the photodiode spectral response which is determined by the device material and geometry can be tailored for specific applications. The device capacitance and carrier transit time are also a function of intrinsic layer width. The optimum compromise between these two characteristics is achieved when the intrinsic layer is such that the transit time is one half of the modulation period [Ref. 17].

The two primary fabrication techniques are the diffusion technique in which a P-type impurity is diffused into an N-type substrate and the Schottky barrier technique in which a thin gold film (about 75 A)) is deposited on the surface of a silicon wafer. Though the device characteristics of each are similar the Schottky device is typically more sensitive in the visible and ultraviolet portion of the spectrum, whereas the planar diffused devices are slightly more sensitive in the IR. Additionally, the diffused devices are recommended whenever high temperatures or high light levels are encountered. Typically planar diffused PIN photodiodes give lowest noise values in small area devices and Schottky photodiodes give lowest noise values in larger area devices.

The avalanche photodiode is very similar to the photodiode mentioned above, except it exhibits current gain through avalanche carrier multiplication. This phenomenon

is observed at high reverse bias voltages where carriers gain sufficient energy to release new electron-hole pairs by collision with valence-band electrons. Substantial current gains, typically 100, are achieved. The highest multiplication is obtained at a bias near the breakdown voltage of the device. Precautions must be taken to circumvent destructive breakdown from temperature variations and bias supply changes. Since the avalanche multiplication is a function of voltage, a well regulated voltage is needed in order to ensure a constant gain with time.

Additional shot noise is introduced by the multiplication process and this imposes a limit on the practical usable gain. However, substantial signal-to-noise ratio improvement is obtained with the avalanche multiplication because the thermal noise of the following amplifier is orders of magnitude greater than the shot noise in the absence of current gain. The largest signal-to-noise ratio is achieved when the device noise equals the amplifier input noise. Economically, the avalanche photodiode is about an order of magnitude more expensive than the PN or PIN photodiodes.

Other possible solid state detectors include phototransistors, photoFETs, and photoSCRs. All these devices are capable of a high gain response but very limited in bandwidth. In general, they can not operate effectively for bandwidths in excess of 10 MHz. Charge coupled devices are also a possibility. Cost is is an important factor for these devices and is prohibitive for most present applications. Yet, they might provide signal processing functions necessary in future systems. Adequate sensitivity and bandwidth will also have to be demonstrated.

It must be noted that photodiode-operational amplifier combinations in the same package are now commercially available at very modest prices. In general, FET operational amplifiers and low-leakage PIN photodiodes are the basic components.

In summary, to the engineer the major characteristics of these depletion mode detectors are the wavelength response, modulation frequency response, and sensitivity. The wavelength is confined between the material bandgap long wavelength cutoff and the recombination limited short wavelength cutoff. In addition to the aforementioned lumped electrical characteristics, the device frequency response is limited by the diffusion effects and drift time in the depletion layer. Because of the low device bulk resistance the ordinary photodiode is thermal noise limited in wideband operation. The following amplifier is the major source of thermal noise. Use of avalanche photodiodes can induce the shot noise to predominate. PIN and avalanche photodiodes are available with bandwidths of above 100 MHz and approaching 1 GHz respectively. For analog applications excellent linearity is afforded by the PIN photodiodes. This is not the case of avalanche photodiodes unless a complex compensating receiver is used to provide a constant and uniform current gain.

III. SYSTEM DESIGN

The basic system architecture proposed was a direct interface of a fiber optics link between an antenna and a receiver. The fiber optic link was designed to insure compatability with a Kollmorgen model 848 voltage probe antenna supplied through the courtesy of the Kollmorgen Corporation and a locally available R-390/URR radio receiver. Basic considerations in the design and construction of the system included the use of commercially available components, economy of cost, compactness of size, and a minimum of system complexity.

The design procedure consisted first of defining the system constraints and secondly of a survey of commercially available products. This concluded with the selection of an LED optical source and a hybrid photodiode-preamplifier detector with similar spectral characteristics compatible with multimode fibers. The basic system components were then designed to achieve the best overall system performance.

A. SYSTEM CONSTRAINTS

Although developed for the specific application cited previously, the fiber optic system is itself a single channel point-to-point wideband communications system. Utility of the system goes beyond the basic demonstrated application. The features of system design were selected to achieve a general overall data transmission objective. In spite of the stress placed on the importance of the coherence of radiation for recent optical transmission systems, an incoherent LED source was used because of the relatively short transmission path and the LEDs high efficiency, compact size, rugged construction, reliability,

and, perhaps most importantly, cost. The ability of the LED to be directly modulated offered the simplest technique for interfacing the fiber optic system and either an analog or digital system using analog intensity modulation and envelop detection of the optical signal. Selection of the LED source dictated a multimode fiber with a relatively large NA-PF combination.

A fiber optics system gives rise to a unique combination of constraints for transmission of analog information. Fundamental and practical differences between optical channels and radio-frequency (RF) channels exist. In optical transmission using an incoherent LED source there is no useful phase information. However, optical direct detection compares rather favorably with heterodyne and homodyne systems since the fiber optics minimizes background radiation noise effects. Gallium arsenide LEDs have output power versus bias current characteristics which are sufficiently linear over a reasonable range that they can be modulated directly by modulating their bias currents. It should be noted that the optical power, not amplitude, is proportional to the drive signal. However, a photodiode detector is a square law device whose output current is proportional to the received power. Therefore, an intensity modulated optical system can be thought of as two transducers converting electrons into photons and vice versa.

The fiber optic communication system developed used a subcarrier direct detection scheme wherein the optical carrier is intensity modulated by a high frequency radio subcarrier wave which is itself modulated by an information signal. Figure 6 contains a generalized block diagram of the receiver section. The output of the optical detector is an electrical signal at the subcarrier frequency plus detector noise. The second detection operation must be performed by the electrical detector to obtain the information signal from the subcarrier. Since the

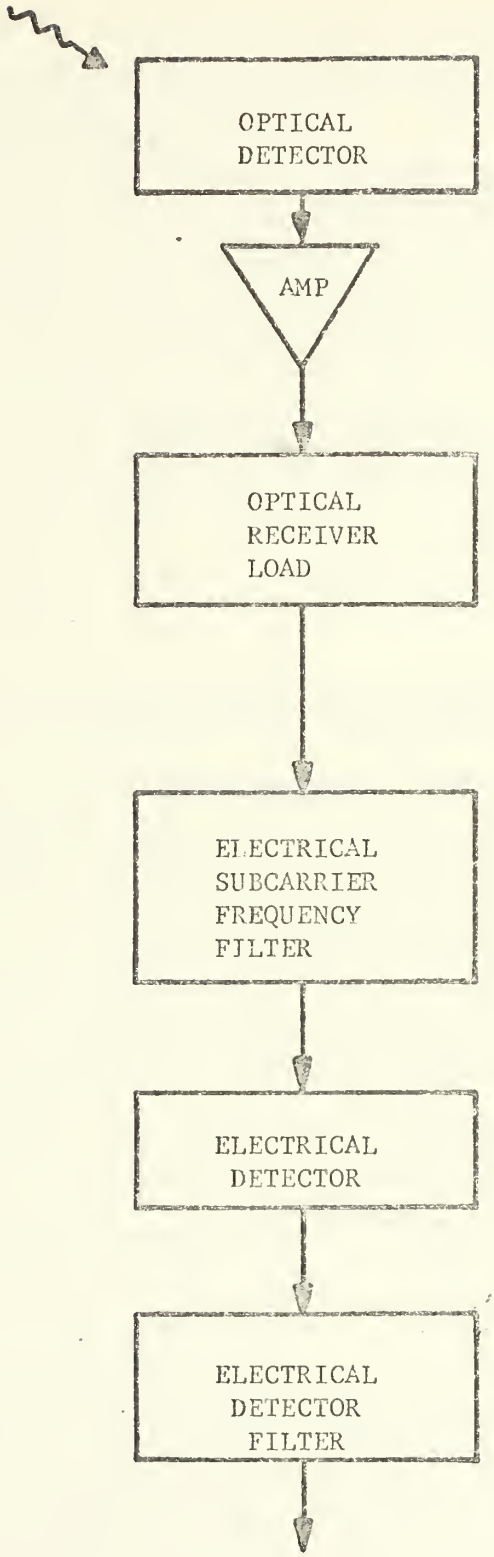

FIGURE 6 SUBCARRIER DIRECT DETECTION OPTICAL RECEIVER

subcarrier filter output voltage is linearly proportional to the subcarrier wave, any linear AM, FM, or PM radio receiver provides proper demodulation.

Development of a suitable design required determination of the critical constraints of the signal-to-noise ratio. Of key importance was the fact that the detected signal is proportional to the square of the modulation index of the sinusoidally modulated carrier, the average received optical power, and the detector efficiency. Provision was made in the design of the modulator to provide for a suitable modulation index while maintaining a satisfactory bias.

B. TRANSMITTER

1. Light emitting diode characteristics

The SPX 1527 stud mounted light emitting diode used in the assembled transmitter is a planar diffused gallium arsenide edge emitter manufactured by Spectronics, Incorporated. Its characteristics are indicated in Table I. The packages have threaded studs and were simply screwed into a common mounting block attached to the printed circuit board which served as a current return path. Figure 7 shows the very narrow, 22 nanometer, spectral emission of the SPX 1527. Figure 8 shows the far-field radiation pattern. The LEDs purchased were selected devices providing a minimum of thirty percent of the total output power in a beam half-angle of ten degrees. Figure 9 shows the forward current-voltage characteristics. Figure 10 shows that the output optical power is linear with bias current in the range of interest with the average optical output increasing about seven percent more than the drive current. The important performance characteristics are the linear output power, radiation response time, and the good thermal design in the LED to minimize junction temperature rise. Since the SPX 1527 is an edge emitter no light comes from the top of

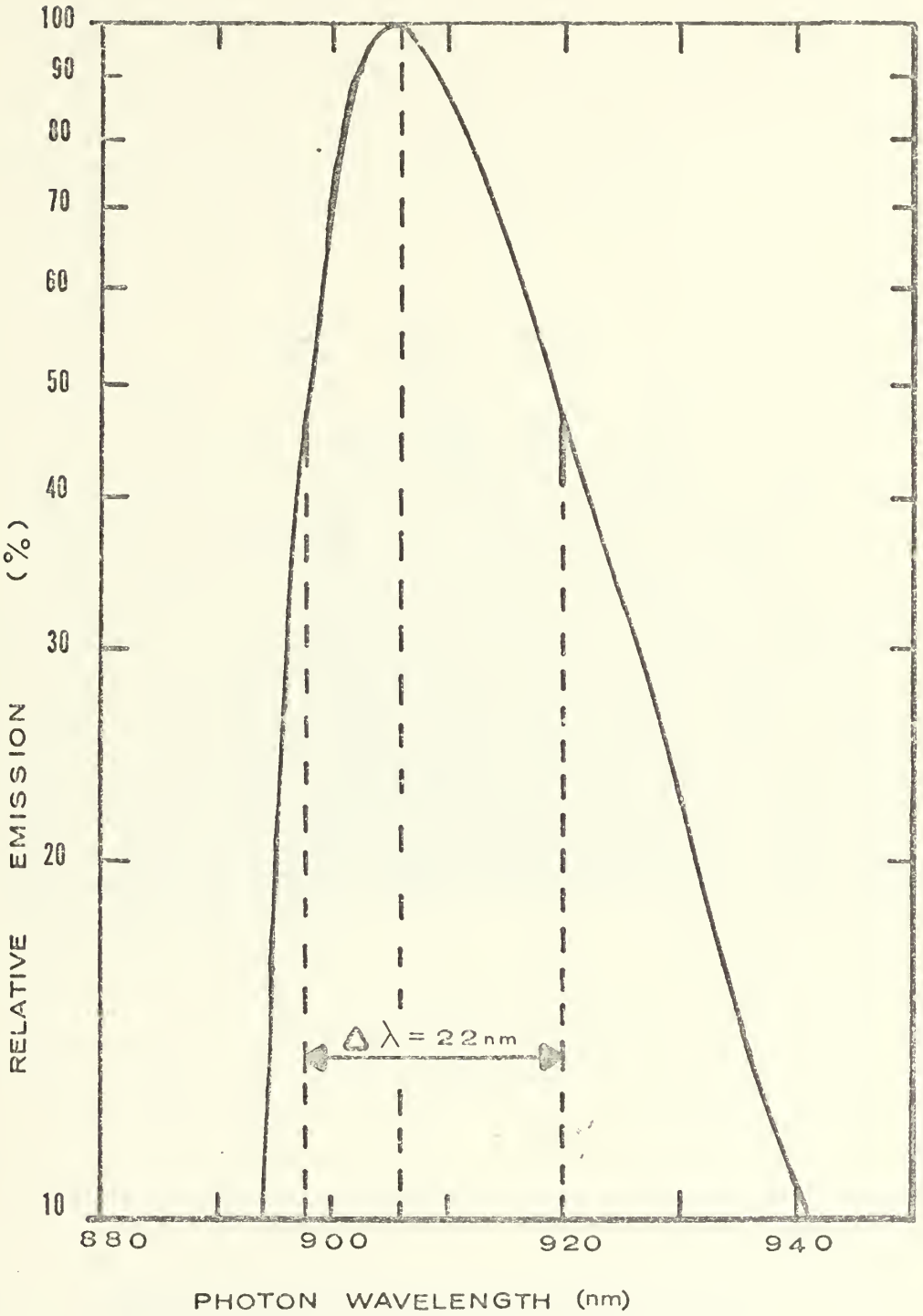

FIGURE 7 SPX 1527 SPECTRAL DISTRIBUTION

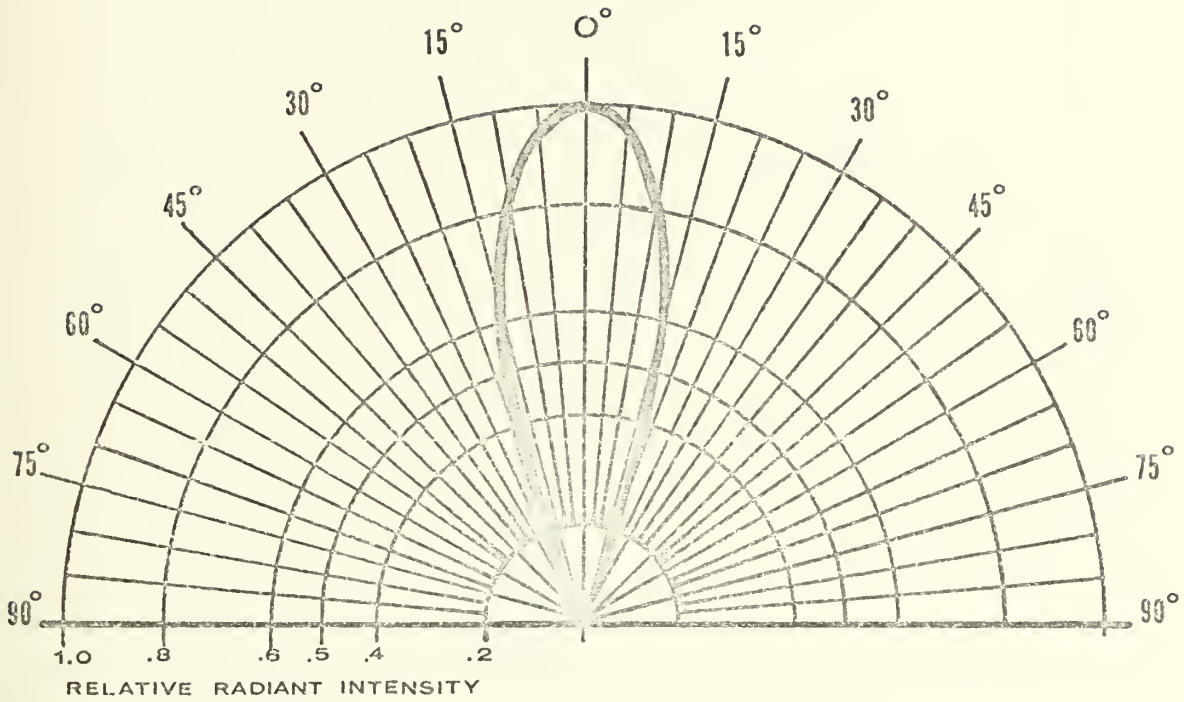

FIGURE 8 SPX 1527 SPATIAL RADIATION PATTERN

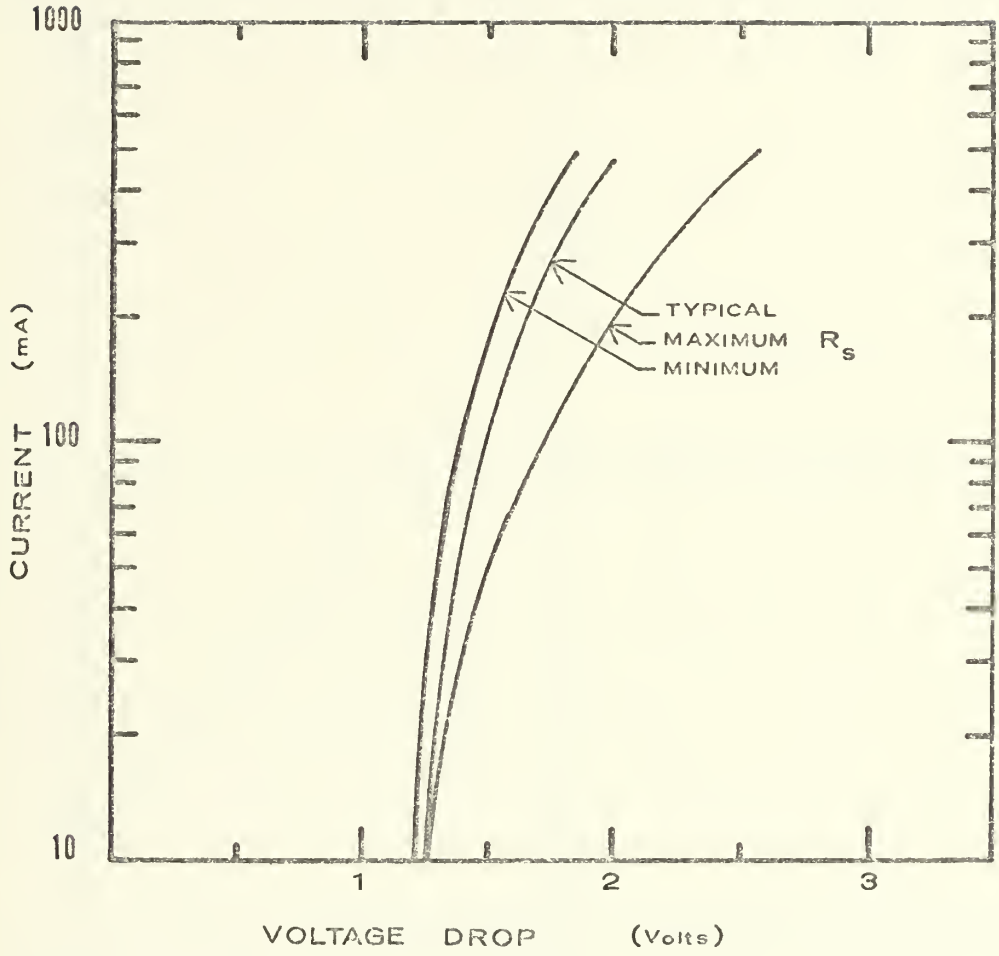

FIGURE 9 SPX 1527 CURRENT VERSUS VOLTAGE

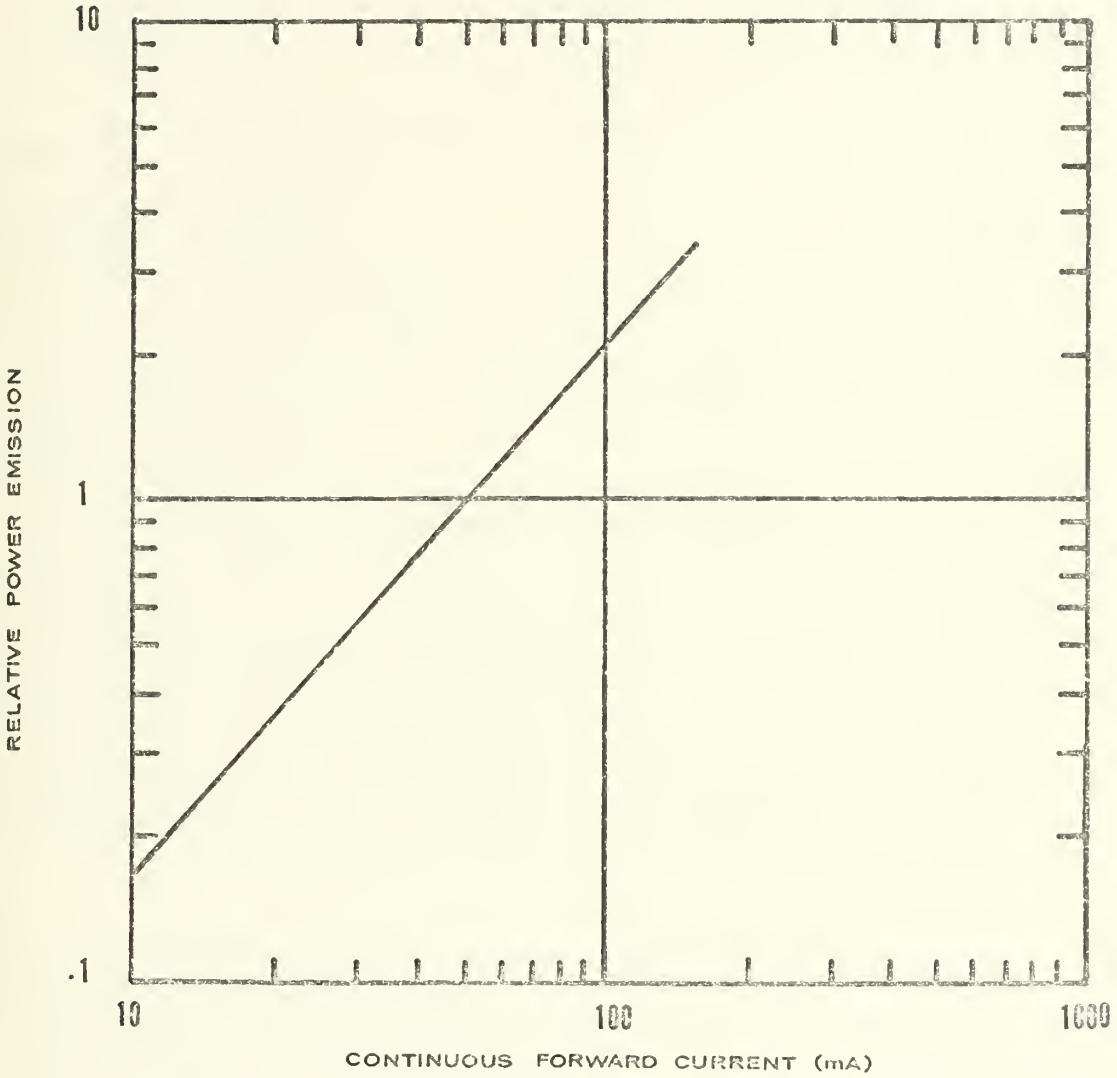

FIGURE 10 SPX 1527 OUTPUT OPTICAL POWER
VERSUS FORWARD CURRENT

Table 1 SPX 1527 LED Characteristics

Parameter	Typical Value
Aperture diameter	.080 in
Junction diameter	.0025 in
Reverse breakdown voltage (I_R = 10 uA)	8 V
Total capacitance (V_R = 1 V, F = 1 MHz)	25 pF
Series resistance	1 ohm
Radiation response time (rise time = fall time)	.02 usec
Delay time	1 nsec
Total power output (I_F = 150 mA)	3 mW
Peak emission wavelength (I_F = 50 mA)	907 nm
Optical bandwidth (I_F = 50 mA, half-power)	22nm

the chip and all light emitted strikes the reflector. Thus the effective emitting area viewed by the fiber is "donut" shaped with a void in the center. The fact that no light will be coupled to the fibers in the center of the fiber bundle is a compelling reason to use a fiber bundle with a sufficiently large numerical aperture for adequate coupling.

2. IED Modulator

In designing a driver circuit for a spontaneous emission source such as an LED, a major consideration is the necessary dc bias current required. Efficient photoemission occurs when the diode is forward biased which then presents

a low non-linear impedance to the circuit. The driver circuit must be designed to limit the diode current and provide adequate thermal stability. Thermal runaway problems which can occur with the use of a voltage supply for current biasing can be avoided by using a current supply which will provide a stable bias and a convenient means for modulation. The linear relation between optical output power and bias current makes spontaneous sources such as the SPX 1527 LED ideal for linear optical intensity modulation.

The driver circuit designed was a two transistor high current gain Darlington pair of emitter followers functioning as a linear amplifier because of the high amount of emitter feedback. The diode bias current was determined largely by the voltage across the two emitter resistors of the second transistor. This voltage was approximately 1.4 volts below the bias voltage established at the base of the first transistor due to the emitter-base voltage drops of the forward biased transistor junctions. The voltage at the base of the first transistor was stable because it was established with a self-biasing resistor network. Hence, the diode bias current was stable. The intermediate resistor in the emitter of the first transistor ensured that each transistor shared in the overall current gain and also reduced the possibility of high-frequency and high-temperature instabilities.

3. Constructed transmitter

A schematic of the total modulator circuit is shown in Figure 11. The first three ac-coupled stages provide the necessary amplification to achieve a suitable modulation index. Because of the wideband requirement it was necessary to select transistors with high gain-bandwidth products to provide gain across the frequency band. The final output transistor also had to be capable of handling the maximum LED bias current of 150 mA. The transistors used were a 3N140 MOSFET input stage, bipolar 2N5835s for the second two

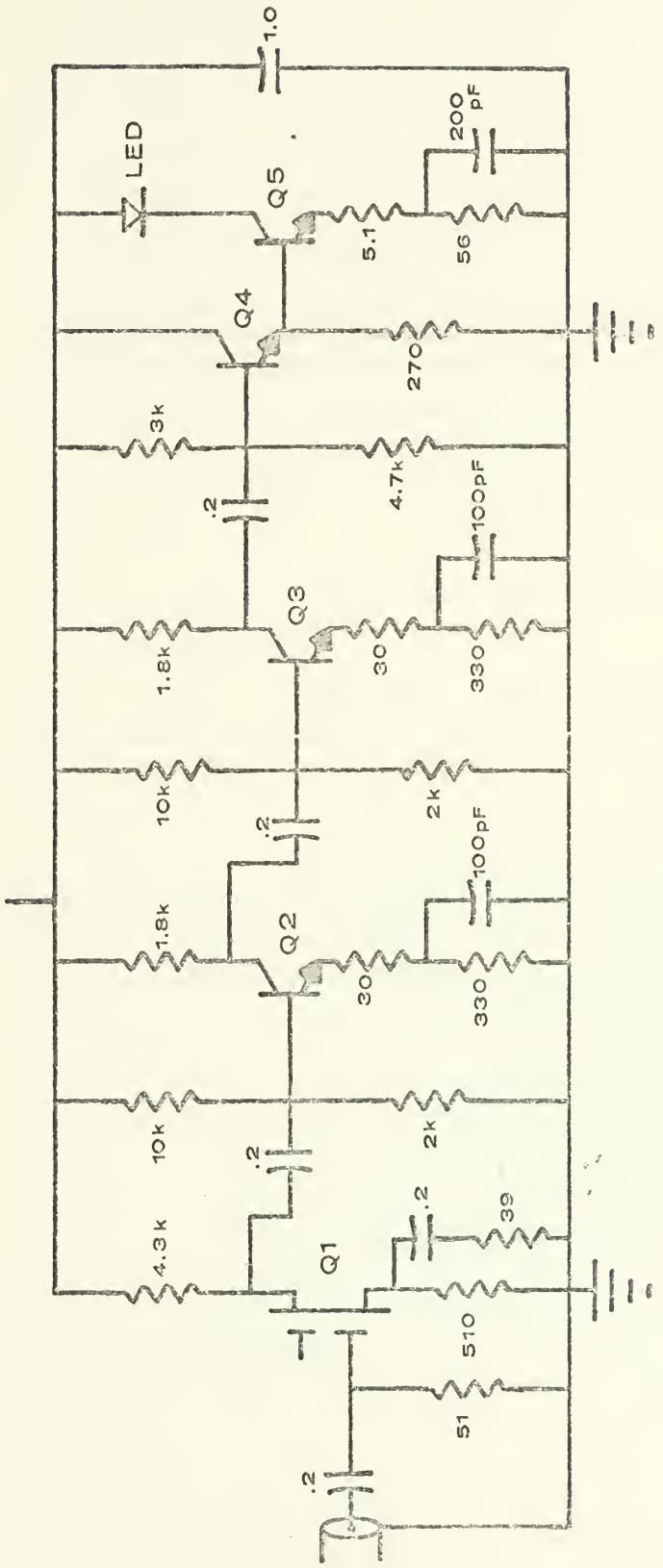

FIGURE 11 OPTICAL TRANSMITTER SCHEMATIC

amplifier stages, and bipolar 2N5109s for the LED driver stage. The 3N140 is a silicon n-channel depletion mode dual-gate MOS field-effect transistor. Primary among the reasons for its use as the input stage was to establish a low noise figure and to minimize cross- and inter-modulation distortion. The 2N5835 is an NPN silicon high frequency transistor with a current gain-bandwidth product exceeding 1 GHz for collector currents of 1 to 10 mA. The 2N5109 is an NPN silicon RF power transistor especially designed to provide large dynamic range, low distortion, and low noise as a wideband amplifier. It has a gain-bandwidth product exceeding 1 GHz over a wide range of collector currents and is capable of handling a maximum continuous collector current of 400 mA. The 3N140, 2N5835, and two 2N5109 output characteristics are shown in Figures 12 through 15 respectively.

Due to the depletion mode operation of the FET, input signals were limited to peak excursions equal to the approximately 0.6 volt source bias voltage. This was compatible with the Hewlett-Packard model HP 461A amplifier used as a pre-amp for the modulator circuit. For other applications where larger input signal levels are available and wider bandwidths desired, a common base bipolar transistor input stage can be used to replace the 3N140 amplifier stage.

A self biasing network was used for the driver biasing. The emitter resistors of both emitter followers established the collector current levels. Analysis of the circuit showed the input impedance to be approximately the parallel base bias resistor combination, R^1. The overall current was approximately the ratio of R^1 to the Q5 emitter resistor. Due to the limitation of the depletion mode operation of the first stage, it was found that the necessary dc bias resistance (Q5 emitter resistor) did not provide the necessary current gain to achieve a satisfactory modulation index. Since a high modulation index was desired

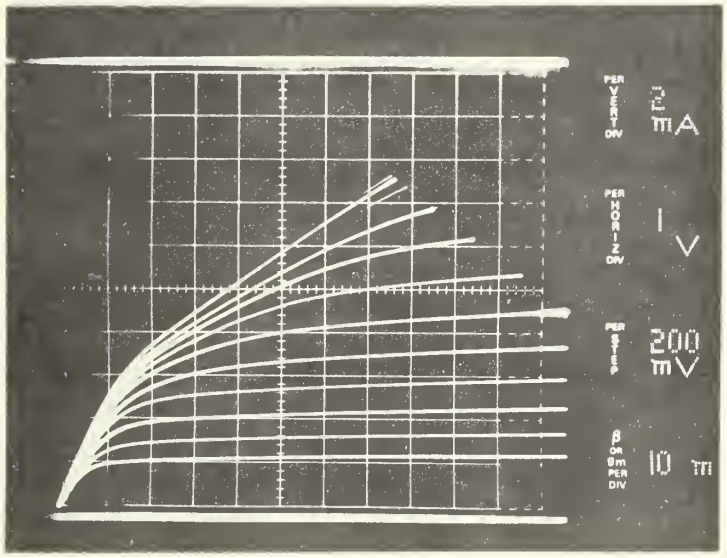

FIGURE 12
3N140 COMMON SOURCE OUTPUT CHARACTERISTICS

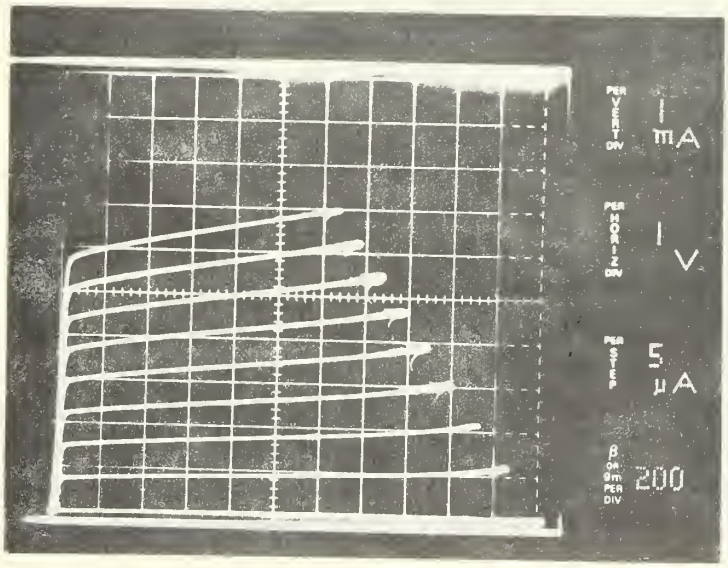

FIGURE 13
2N5835 COMMON EMITTER OUTPUT CHARACTERISTICS

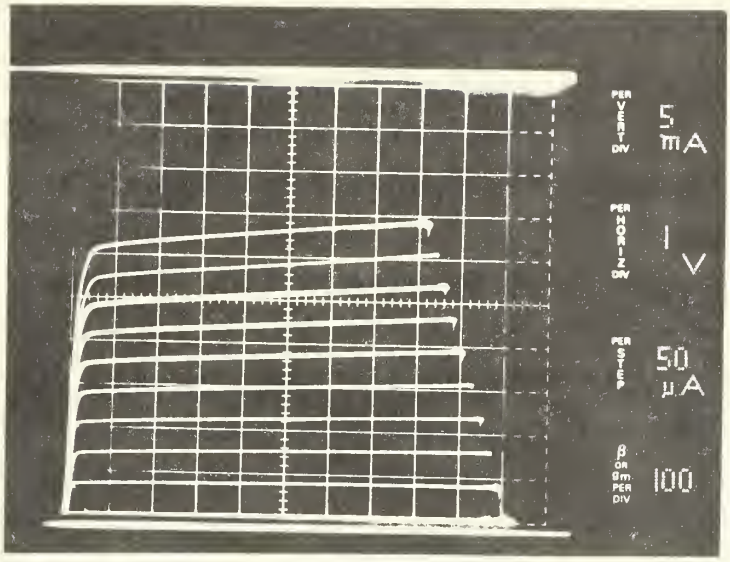

FIGURE 14
Q4 2N5109 COMMON EMITTER OUTPUT CHARACTERISTICS

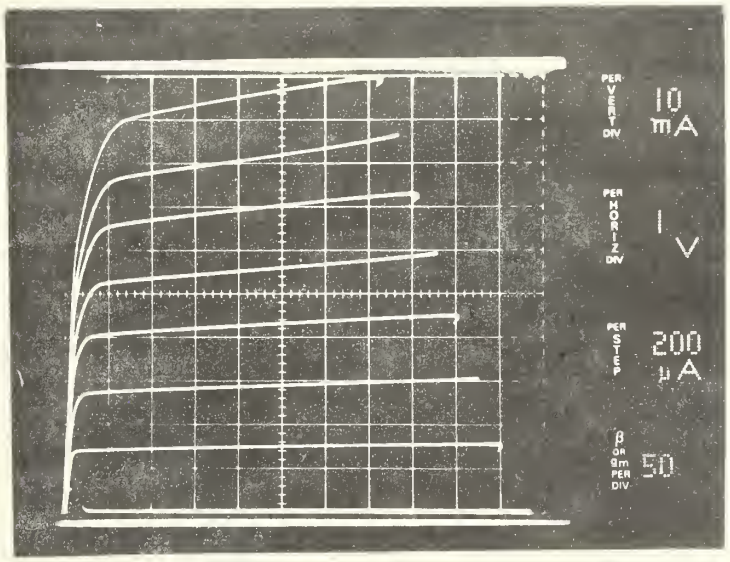

FIGURE 15
Q5 2N5109 COMMON EMITTER OUTPUT CHARACTERISTICS

for increased signal-to-noise ratios at the detector it was necessary to avoid the degeneration and hence loss of current gain due to the Q5 emitter resistance. Since the total dc resistance was determined from bias conditions, the effective ac emitter resistance was lowered with a by-pass capacitor shunting a portion of the dc resistance. This result is indicated in the schematic.

The LED bias current level was set at slightly above 70 mA which was the collector current producing optimum gain-bandwidth performance of the 2N5109. Operating at this current level necessitated placement of a heat sink on the output transistor for improved heat dissipation. The total power supply requirements for the transmitter are a positive 12 volts delivering 115 mA.

The modulator was fabricated on a 3 by 5 inch two-sided printed circuit (PC) board and mounted in a metallic box. The box used had louvered side vents to provide adequate ventilation. Ground planes were established on each side of the PC board and connected to chasis ground through the four corner supports. In addition, component ground connections were soldered on both sides of the PC board to equalize the potential at all points in both ground planes. External power supply terminals and a BNC input connector were used to eliminate spurious radiations. Proper layout and shielding of the transmitter was necessary to realize the full potential of the RFI and EMI characteristics of the fiber optics.

A plugable connector for the fiber was machined locally to provide a firm mounting support and provide coupling ease for the fiber bundle. Similar to a "phono jack", a female receptacle was wall mounted in both the transmitter and receiver boxes. Both ends of the fiber were fitted with male connectors. These connectors consisted of a retainer collar holding a split cylindrical collar around the ferruled fiber ends. The retainer collar and top of the split cylindrical fiber collar can be seen in Figure 16

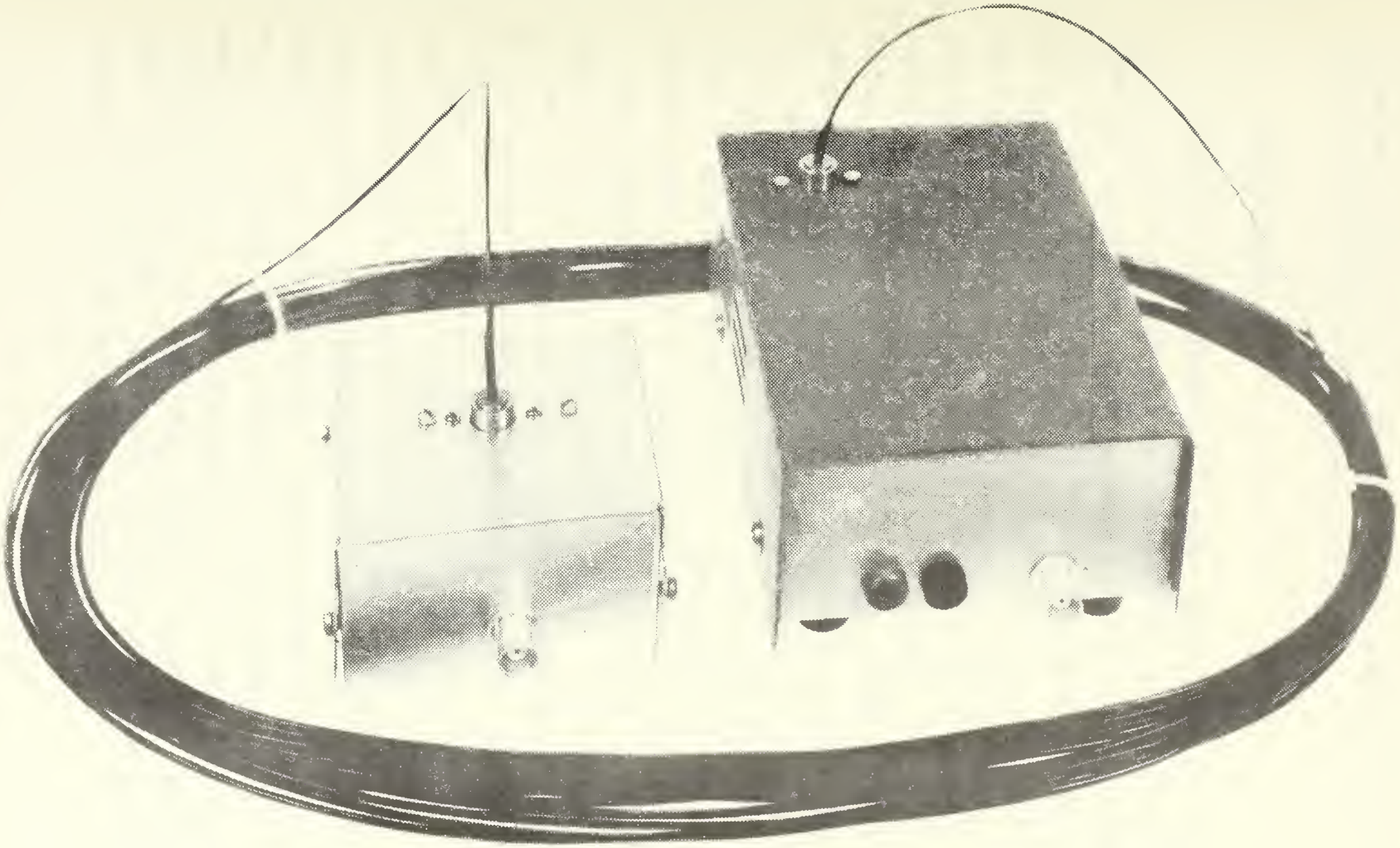

FIGURE 16 OPTICAL INTERFACE

which shows the optical transmitter, fiber, and optical receiver combination. Though simply designed and fabricated these connectors worked quite well.

C. OPTICAL FIBER

During development of the fiber optic system total optical attenuation was an important design parameter in specifying system performance and device selection. Since the total permissable attenuation can be increased only by increasing the total optical power from the LED or by increasing the photodetector responsivity, design flexibility was limited. In the system developed the fiber optics contributed most of the optical attenuation. The fifty foot, lens terminated fiber optic bundle used was purchased from Spectronics Incorporated with the designation SPX 1633. The fiber optic bundle was made from conventional multimode fibers manufactured by Galileo Electro-Optics Corp. and lens terminated by Spectronics. Characteristics of the Galileo fiber bundles are shown in Table 2. Choice of the relatively high loss fibers was due to the relatively short transmission path which caused the primary optical losses to be due to coupling and decoupling light from the fiber bundles. Low-loss fiber bundles with their poor packing fractions and low numerical apertures impose coupling penalties which, for short distances, does not justify their choice over the more economical conventional fiber optics. Comparing the Corning Glass low-loss fiber bundles to the Galileo fiber bundles showed a NA of .14 versus .66 and PF of .27 (-5.7 dB) versus .75 (-1.3 dB) respectively. The difference in the packing fraction introduces a 4.4 dB comparative coupling penalty. The total attenuation for the 50 foot cable used was 12 dB as compared to 1.5 dB for a low-loss cable.

Table 2 Fiber Optic Characteristics

Individual fibers	Nominal value
Outside diameter	.0025 in
Core to outside diameter ratio	20/21
Numerical aperture	.66
Core index	1.625
Fiber optic bundle	
Bundle diameter	.045 in
Outside diameter	.088 in
Packing fraction	.744 (-1.29dB)
Jacket material	PVC
Attenuation	-.24dB/ft

The lens terminations with the fiber at the focus eliminates the void in the near field SPX 1527 radiation pattern and uniformly illuminates the end of the fiber as shown in Figure 17. The fact that the lens diameter is 1.75 times larger than the LED reflector aperture makes the coupling loss insensitive to small changes in the lens and LED relative positions.

Preliminary design work was made using the following assumed system optical attenuation sources: LED (10° half

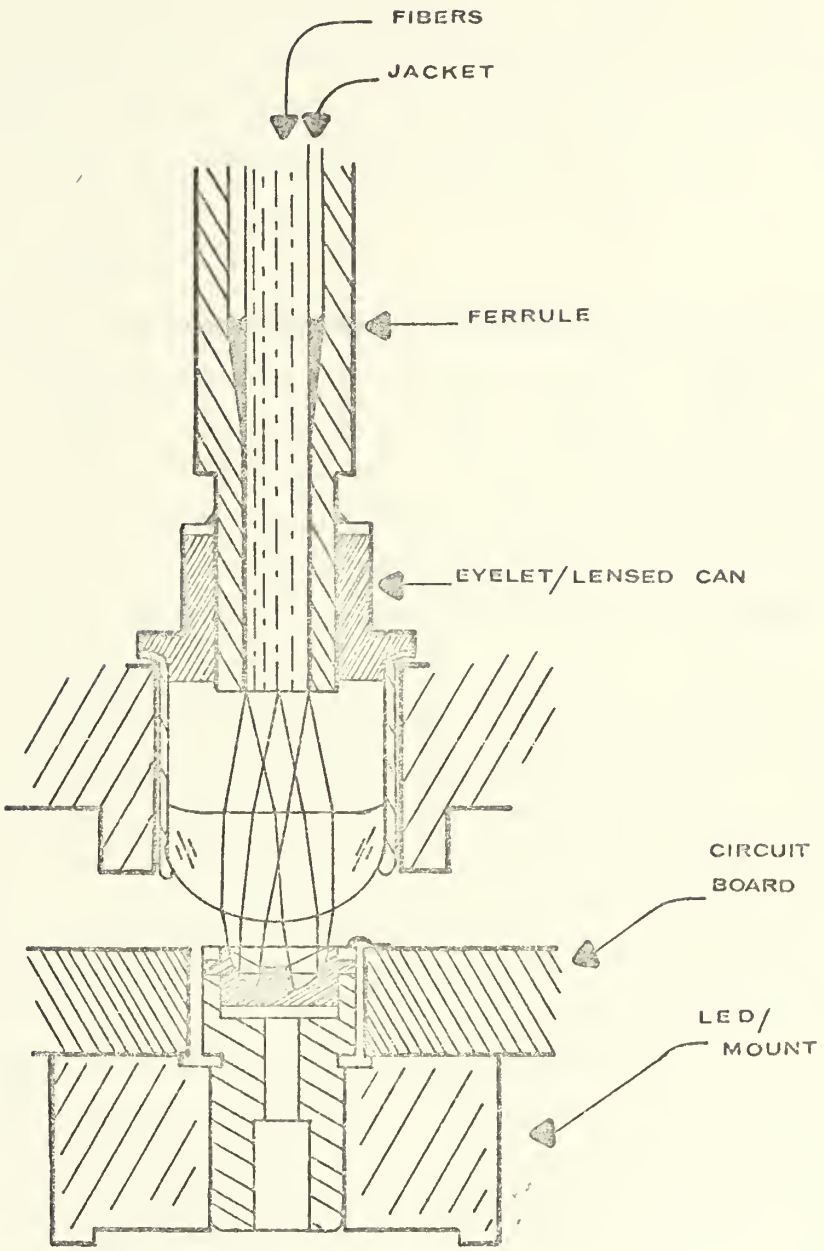

FIGURE 17
LED-FIBER INTERFACE

angle), -5 dB; LED/fiber interface, -3dB; fiber bundle, -12dB; detector/fiber interface, -3dB. This resulted in an assumed total system attenuation of 23dB. The system attenuation was measured using an insertion loss technique. This measurement was made using the SPX 1527 and the MDF 428 under the same operating conditions as used in the communications system.

D. OPTICAL RECEIVER

Performance and economic considerations prompted the choice of a PIN photodiode for the optical detector. To minimize interface complexity and ensure best operating performance of the photodiode, a photodiode-preamplifier combination was selected. This device, one resistor, and two capacitors provided a direct interface with the R-390/URR radio receiver which was easily implemented and efficient in operation.

The photodetector selected was a MDF 428 manufactured by Meret Inc. This high speed hybrid optoelectronic receiver is a silicon PIN photodiode-transimpedance amplifier combination in a single 3-pin TO-5 header package. The MDF 428 offered a spectral responsivity shown in Figure 18 which provided excellent compatability with the SPX 1527 plus a nominal electrical bandwidth of dc to 60 MHZ. The maximum responsivity of 4.5 mV output per microwatt of incident optical power occurs at 905 nm. The device output rms noise voltage in a 50 MHz bandwidth is less than 80 microvolts and the noise equivalent power (NEP) per root Hertz is 10^{12} Watts/(Hz) . Power supply requirements are a single B+ (from +3 to +12 volts) at a current drain of less than 3.5 mA. The single power supply provides bias for the PIN photodiode and operational voltage for the transimpedance amplifier. Figure 19 shows a schematic of the detector/amplifier combination.

E. INTEGRATED SYSTEM

The integrated system configuration with the fiber optic

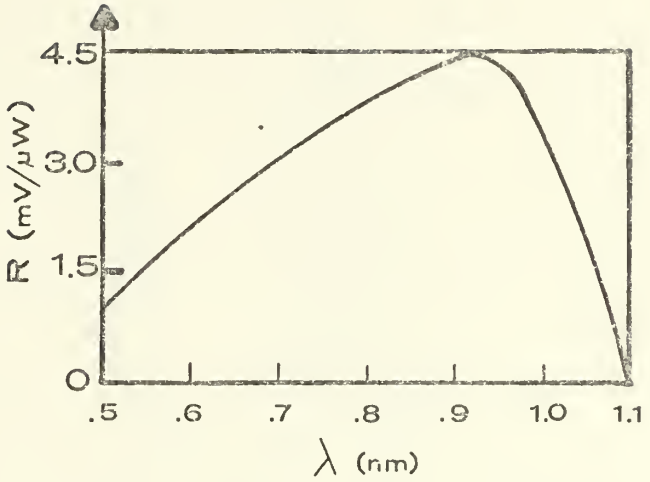

FIGURE 18
MDF 428 SPECTRAL RESPONSIVITY

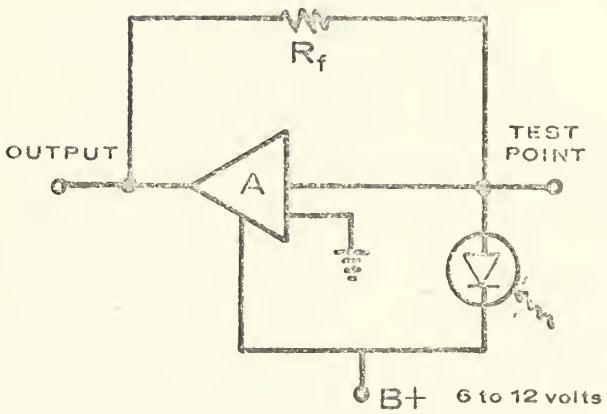

FIGURE 19
PHOTODETECTOR SCHEMATIC

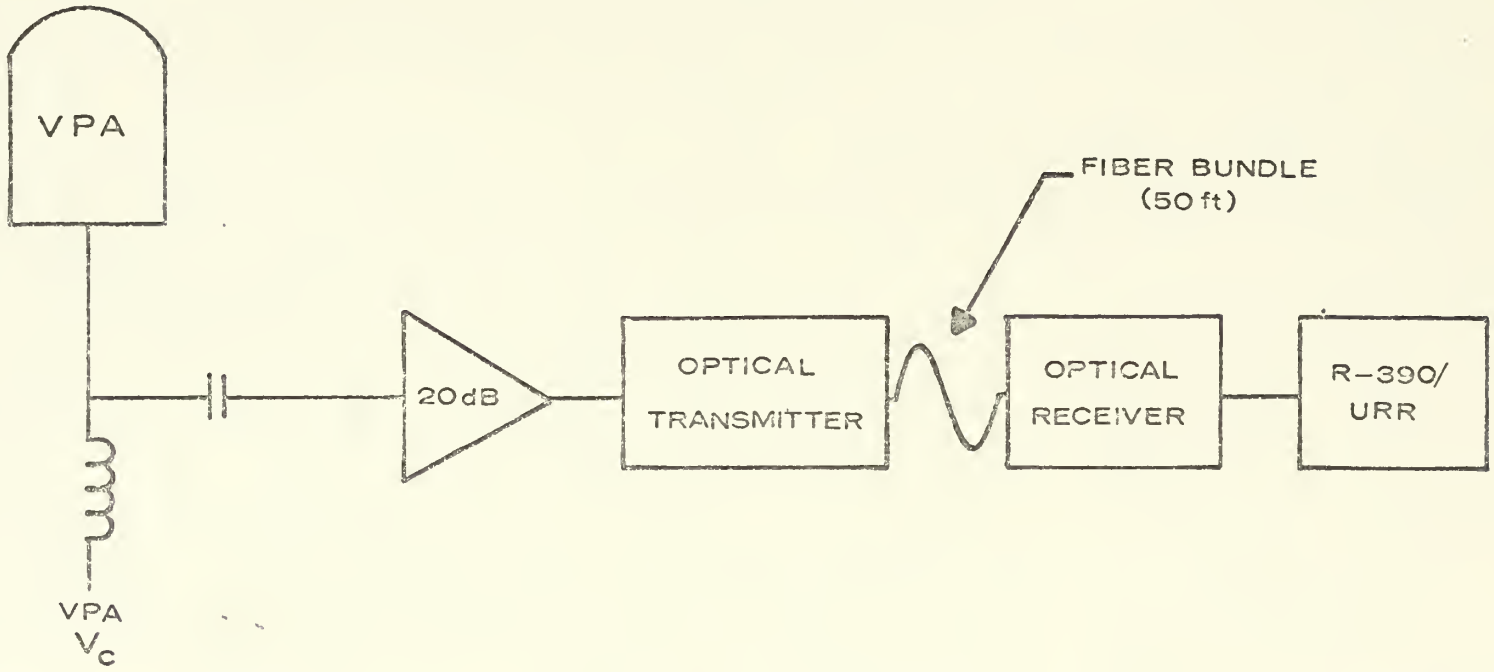

FIGURE 20 INTEGRATED SYSTEM

interface is shown in block form in Figure 20. It was a direct fiber optic interface between the VPA antenna and the R-390/URR radio receiver. All system components preceding the receiver were in wideband operation and passed RF high frequency (HF) signals from 0.5 to 32 MHz.

The Kollmorgen voltage probe antenna is a very compact broadband antenna. The entire package is cylindrically shaped with a diameter of two inches and a height of three inches. A schematic of the VPA is shown in Figure 21. Power (28 V dc) was supplied to the VPA through the inner coaxial line conductor.

Due to the low output signal levels from the VPA it was necessary to provide amplification to achieve signal levels adequate to drive the LED driver stage. The Hewlett-Packard model 461A wideband amplifier was used as a 20 dB pre-amplifier for the optical transmitter. It has a frequency response of ±1 dB from 1 KHz to 150 MHz. Although a 40 dB gain mode was available, the maximum output of the 461A was 0.5 V rms or 1.4 V peak-to-peak. Using these values, the maximum input signal, without clipping, is 140 mV and 14 mV on the 20 and 40 dB gain modes respectively. The depletion mode operation of the input stage of the transmitter limited its input to 620 mV. It was determined that local commercial AM radio signals were of sufficient strength to saturate the input stage in the 40 dB mode. Consequently, the 461A was operated exclusively in the 20 dB mode throughout the test and analysis procedures.

The R-390/URR has been the primary military general purpose HF receiver for two decades. It provides for the reception of voice, CW, single side band, and frequency-shift signals over a frequency range of 0.5 to 32 MHz. The receiver is a thirty-two tube, twenty-six crystal, superheterodyne receiver of the triple conversion type. Triple conversion is used for the lower frequencies (to 8 MHz) and double conversion for the higher frequencies (8 to 32 MHz).

The receiver furnishes audio frequency (AF) output power to a local headset and/or speaker. A 455 KHz intermediate frequency (IF) output is also available to drive auxilliary equipment. Both were used in the overall system test and evaluation.

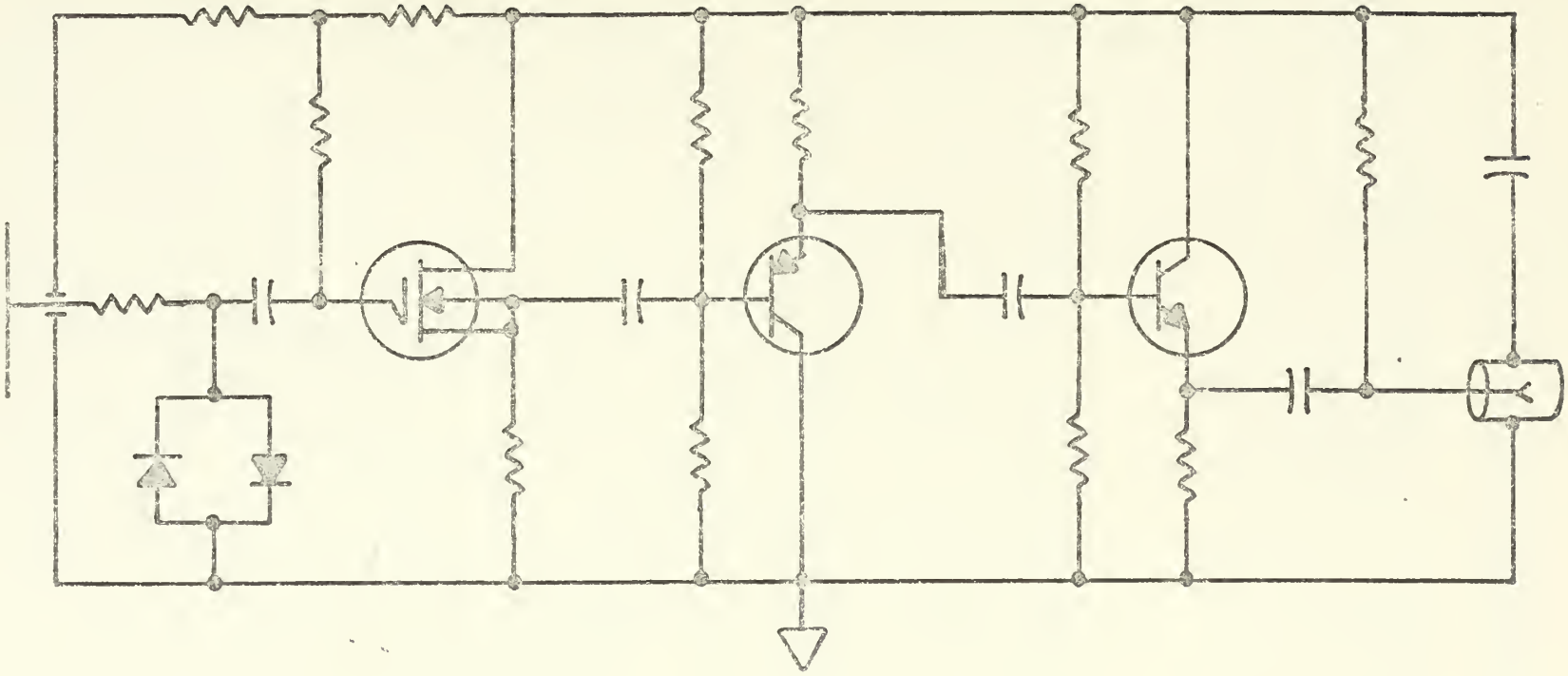

FIGURE 21 VPA SCHEMATIC

IV. SYSTEM PERFORMANCE

Tests were performed to determine the complete integrated system performance. Analysis of the system consisted of an examination of its frequency response, minimum discernible signal, saturation level, and distortion characteristics.

A. FREQUENCY RESPONSE

Due to the upper frequency rolloff gain characteristics of the VPA the frequency response of the optical transmitter was tailored to partially compensate for this fact and to compensate for the proximity of a local commercial AM radio transmitter transmitting at 1.24 MHz.

The voltage response of the transmitter was examined with the test configuration shown in Figure 22. Equipment used in this and subsequent tests included an SG-85/URM-25D RF signal generator, MX-1487/URM-25D impedance adaptor, and a Tektronix type 422 oscilloscope. Instruments were interconnected with five feet lengths of RG-58C/U coaxial cables with BNC terminations. Hewlett-Packard 621A power supplies were used to provide power to both the optical transmitter and receiver. The voltage response test was conducted by inserting a constant 5 millivolt peak-to-peak sinusoidal input and measuring the Q5 emitter voltage. The input and output signal levels were continuously monitored on channels 1 and 2 of the oscilloscope respectively. The voltage response is shown in Figure 23. Tailoring of this response was accomplished by the selection of the emitter by-pass capacitors in the three amplifier stages.

The optical system response was performed using the configuration shown in Figure 24. A second 461A amplifier was used to drive the oscilloscope due to the receiver

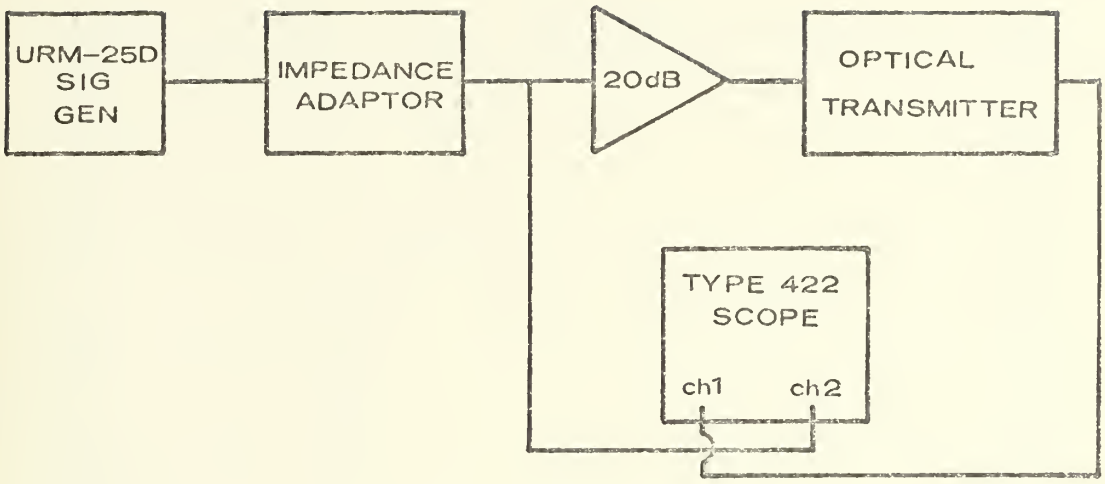

FIGURE 22 VOLTAGE RESPONSE TEST EQUIPMENT CONFIGURATION

FIGURE 23 TRANSMITTER VOLTAGE RESPONSE

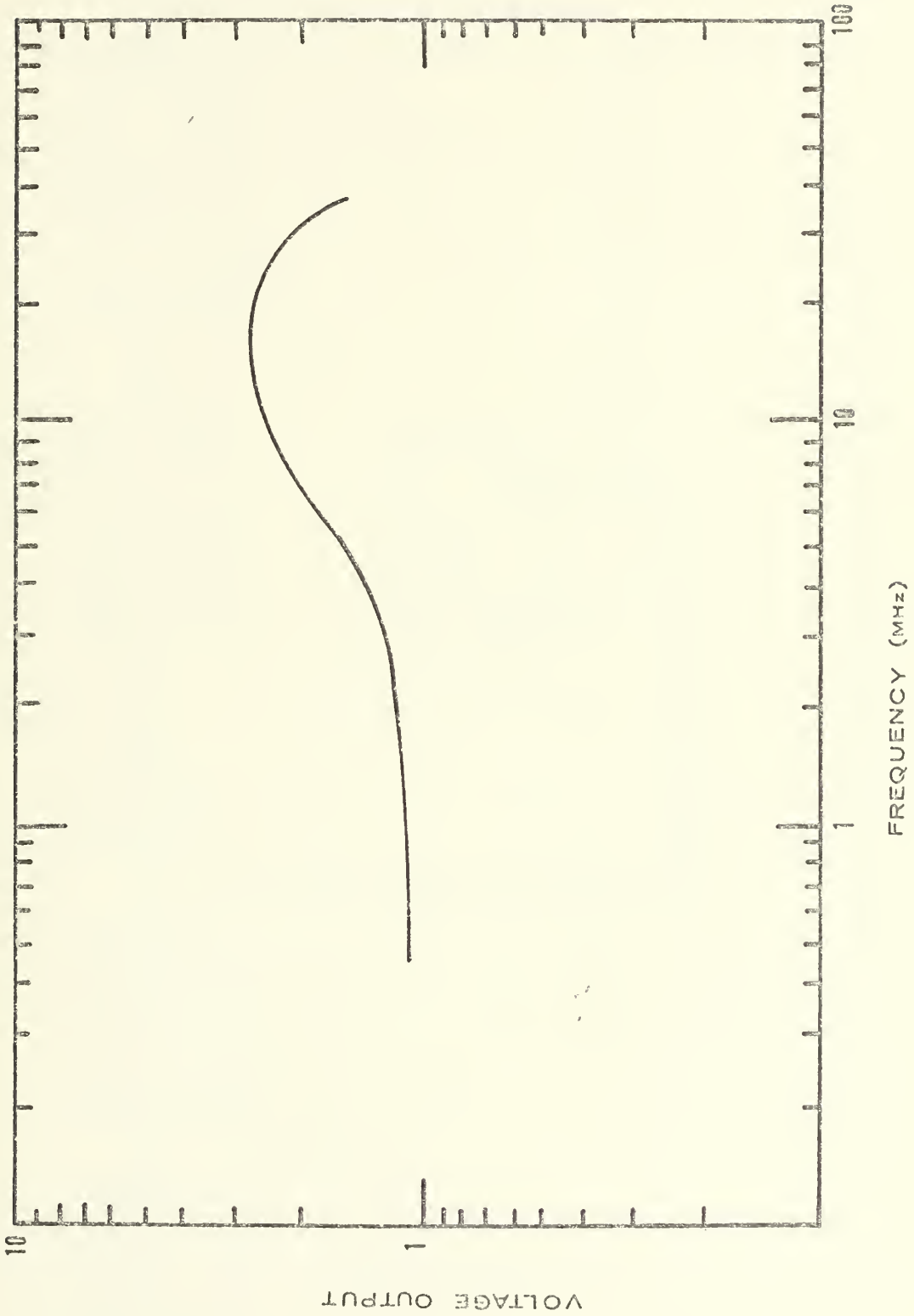

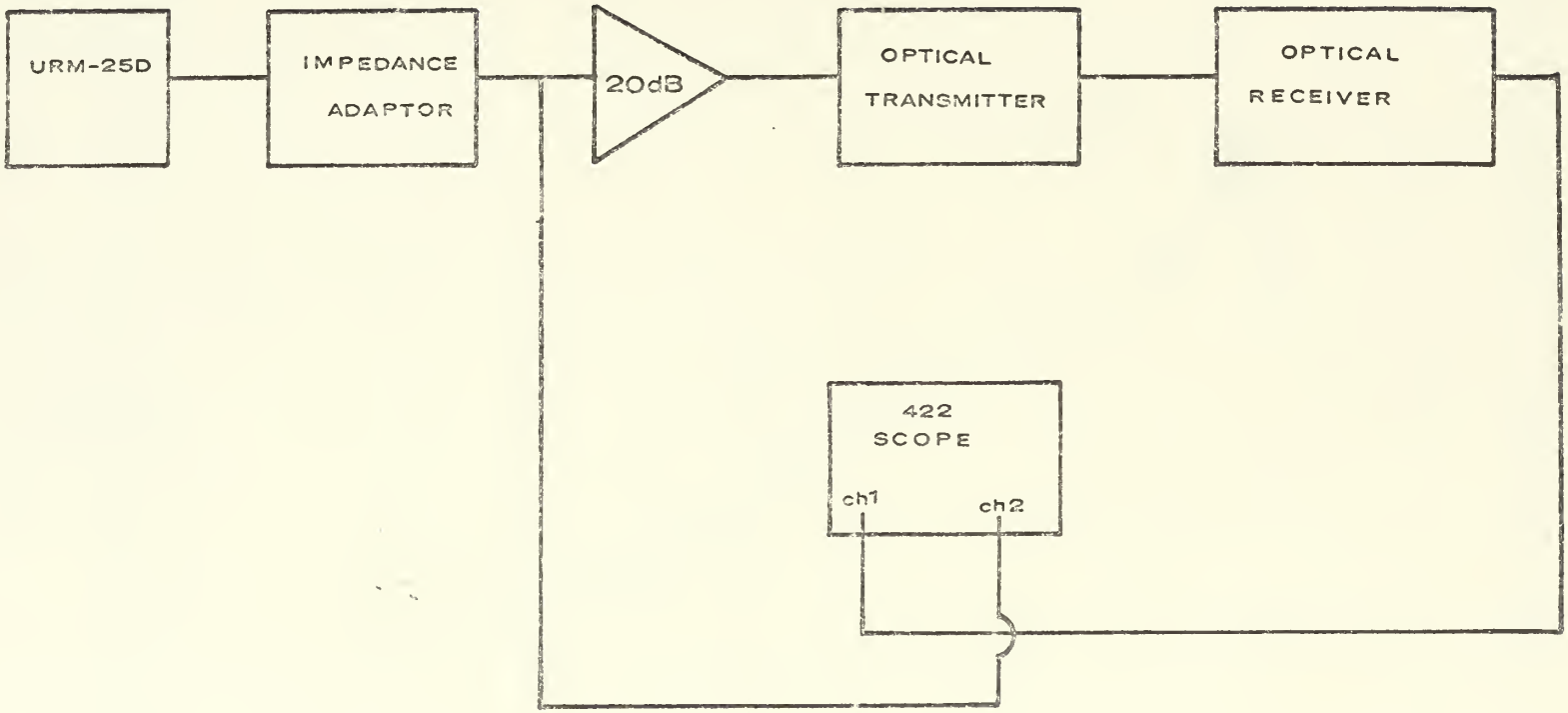

FIGURE 24 OPTICAL SYSTEM PERFORMANCE TEST EQUIPMENT CONFIGURATION

FIGURE 25 OPTICAL SYSTEM RESPONSE

output signal level. The results are indicated in Figure 25. The low frequency response was suppressed by the Q5 emitter by-pass capacitor. This proved the best choice to compensate for the local signal environment. However, only one gate of the dual-gate 3N140 was used in the constructed transmitter. Use of the second gate of this device could also provide compensation. This extra design flexibility was incorporated for future refinements of the system.

The operational frequency response of the complete interfaced receiver system was determined using the configuration of Figure 26.. The "phones" AF output was used to drive the 422 oscilloscope for measurement purposes. Figure 27 indicates the results of this test.

B. MINIMUM DISCERNIBLE SIGNAL

Determination of the minimum descernible signal (MDS) level was conducted over the HF band by means of the audio output of the R-390. The phone AF output monitored aurally on a standard 600 ohm headset and the IF output visually on a Tektronix type [illegible] dual-beam oscilloscope with a type 1L5 spectrum analyzer plug-in unit. The R-390 receiver was operated with maximum RF gain, maximum local AF gain, 1 KHz bandwidth, and in the manual gain control mode. The BFO was used to provide an audible AF output. The MDS was one microvolt for the 2-25 MHz band and a maximum of three microvolts across the total band. In all cases the fiber was disconnected to ensure it was conducting the signal.

C. SATURATION LEVEL

It was experimentally verified that the depletion mode operation of the input stage established the system saturation level. An input voltage of 62 mV to the 461A preamplifier was sufficient to saturate the optical transmitter and introduce severe distortion. Observations of the AF output indicated that proper adjustment of the RF

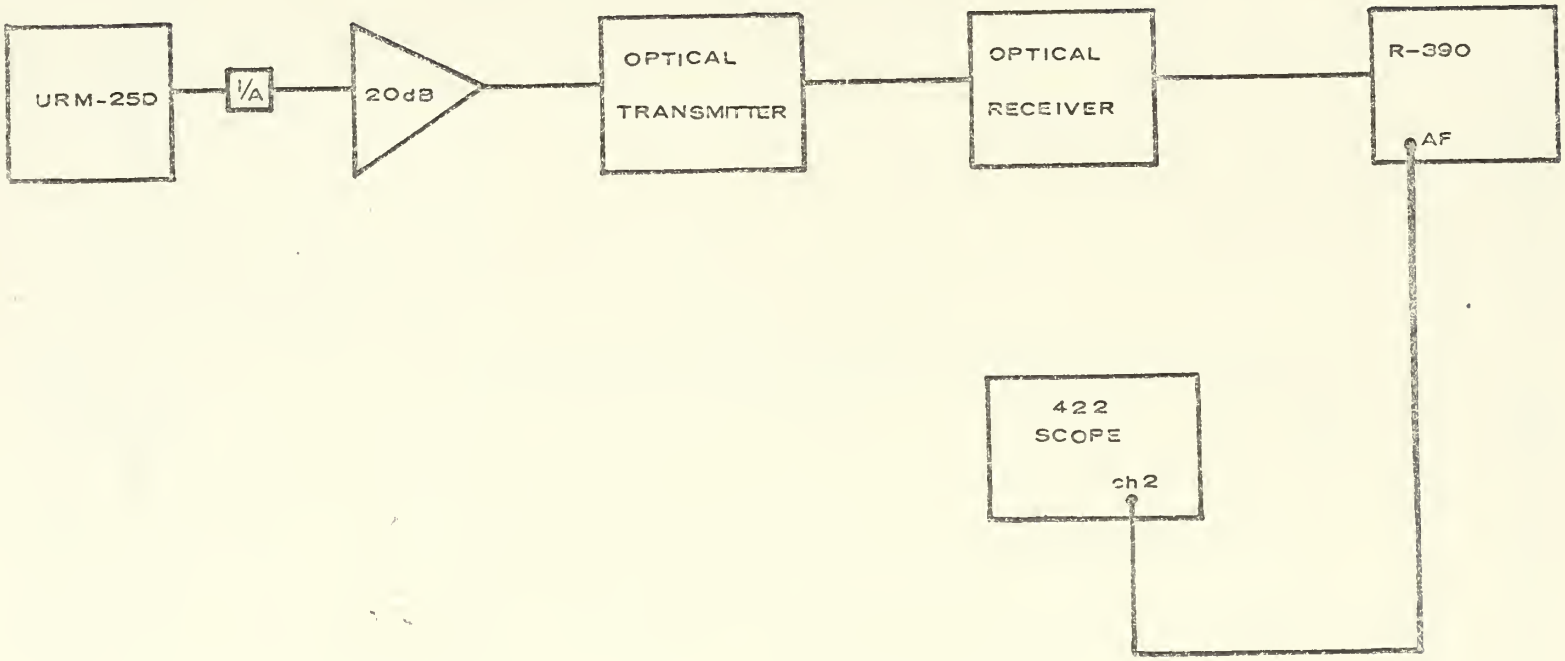

FIGURE 26 INTEGRATED RECEIVER SYSTEM TEST EQUIPMENT CONFIGURATION

FIGURE 27 INTEGRATED RECEIVER SYSTEM RESPONSE

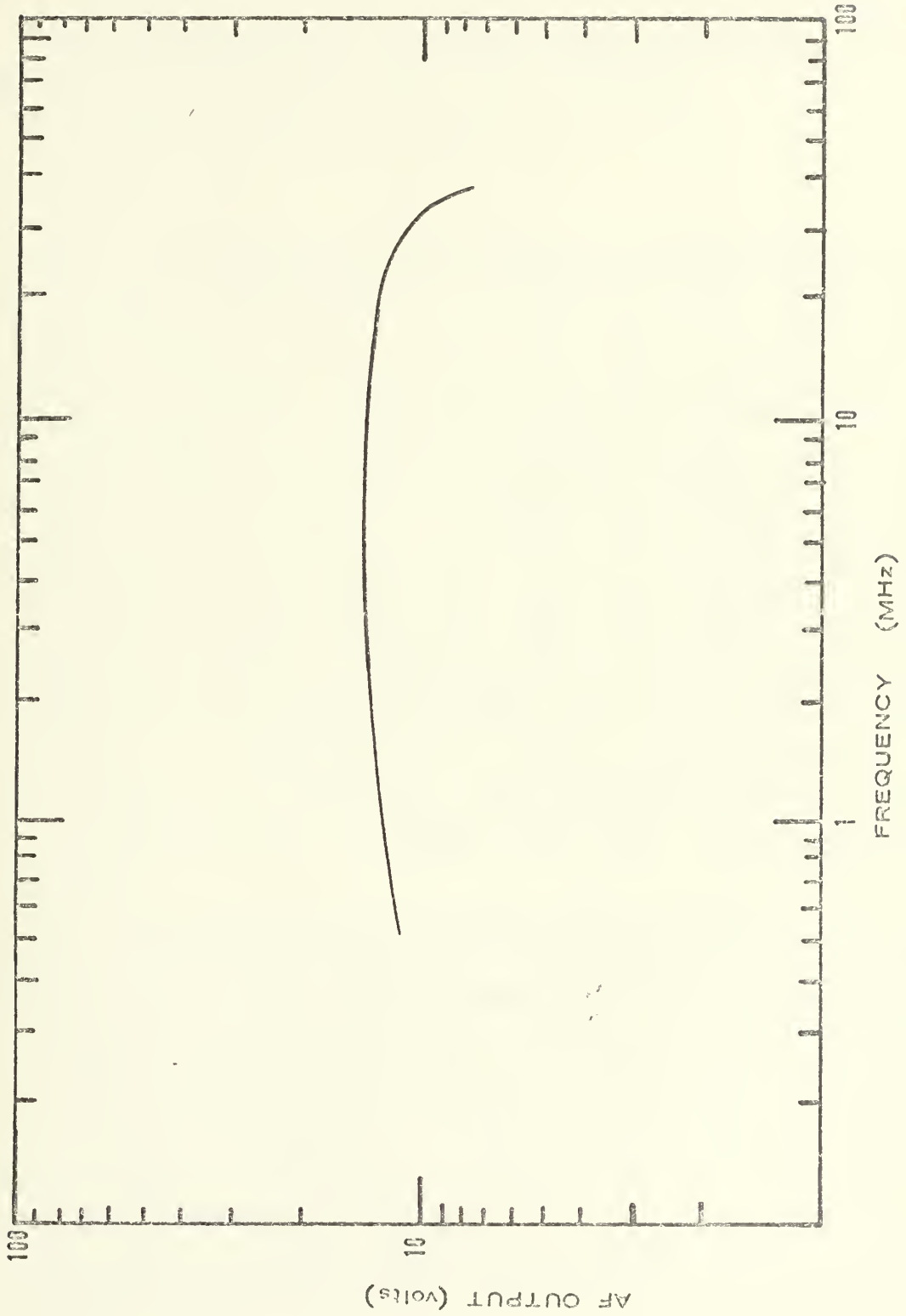

gain and AF local gain controls on the R-390 was necessary to prevent saturation of the AF output for millivolt input signal levels.

The dynamic range of the system can be determined from a comparison of the system MDS and saturation level. The mid-band dynamic range was in excess of 80dB.

D. DISTORTION

Tests were performed to determine the distortion levels of the system. No harmonic or inter-modulation distortion was observable in the IF or AF output of the R-390. Therefore, the optical receiver output was sampled directly. Signal content of the fundamental and in-band harmonics of a 1 mV, 5 MHz input signal was determined with the aid of the Tektronix 551 dual-beam oscilloscope/1L10 spectrum analyzer plug-in unit combination. A 461A 40dB instrumentation amplifier was used to amplify the optical receiver output and drive the spectrum analyzer. The input signal was first monitored to establish a reference level for the fundamental and harmonics of the URM/25D signal generator output. These were used to normalize the observed system output. The first harmonic was 45 dB below the fundamental signal level All harmonics were a minimum of this value below the fundamental.

The intermodulation distortion level resultant from the product of two input signals was determined. A 5 MHz signal was obtained from the SG-85/URM25D and a 7 MHz signal from a SG-117/URM26D signal generator. Again, the input signal was monitored to normalize the system output. For signal input levels from 1 microvolt to 10 millivolts the output inter-modulation frequency outputs are a minimum of 40 dB below the fundamental outputs.

The above results indicate no appreciable distortion introduced by the fiber optic interface.

V. CONCLUSIONS AND RECOMMENDATIONS

This project consisted of essentially two primary thrusts; the status of present optoelectronic technology and its applicability to a specific problem. It was found that, indeed, the present optoelectronic and fiber optic technologies are sufficient for the development of first generation systems using discrete components and multimode fibers. Many near term applications capitalizing on the inherent advantages of the fiber optics transmission medium have already been explored and implemented by government agencies as well as commercial concerns. In most cases, off-the-shelf fiber optics and discrete components have been utilized. These efforts directly reflect the recent trends in modularization, digitalization, and miniaturization.

A preliminary effort was made to determine the applicability of fiber optics technology to the antenna-receiver interface in a radio system. An interface was designed, fabricated, and tested. It is felt that the proposed direct interface in a receiver system requiring high sensitivity, large dynamic range and low distortion presents a dilemma with the present semiconductor technology. The maximum linear dynamic range of the LED optical sources is confined by their power dissipation ratings and temperature effects. The required sensitivity would dictate the use of an avalanche detector which is a non-linear device unless intricate compensation is provided. Hence, a distortion problem. The PIN photodiode solves the distortion problem but at the expense of a restricted dynamic range. The dynamic range of the MDF 428 was specified by the manufacturer at slightly over 40 dB. However this specification is for a wide band measurement instrument. The performance of the developed interface clearly indicates that a narrow band detector such as the

R-390 can significantly extend this range. It was learned subsequent to the construction of the optical interface that Meret has developed another photodetector (MDF 528) providing an additional 10-15 dB dynamic range. This was accomplished by providing separate power supplies for the PIN photodiode and the transimpedance amplifier.

While facilities for comprehensive testing of the integrated system with calibrated antenna inputs was not available, serveral conclusions have been reached from the bench testing done. The basic concept of the interface for an HF system of an analog intensity modulated LED, conventional multimode fiber optics, and photodiode detector has been demonstrated. The SPX 1527 radiation response time of twenty nanoseconds will prohibit its use at higher frequencies. This fact is true for present commercially available LEDs. The interface complexity could be significantly reduced by direct incorporation of an LED within the VPA antenna. The circuit of the VPA would require only minor modification. This is an engineering practicality and certainly far superior to the developed system. In addition, this would provide an optoelectronic interface consistent with military requirements that is potentially much superior to present techniques.

For shipboard and avionic applications, notably where many sensors are co-located, data transfer from sensor to detector will be facilitated in the future by a fusion of existing single mode fibers, current avionic data-bus technology, the emerging integrated optics technology, and improved optical modulation techniques.

REFERENCES

1. Nuese, C. J., Kressel, H., and Ladany, I.,"The future for LEDs", IEEE Spectrum 9:28-38, May 1972.

2. Smith, R. G., "Optical power handling capacity of low loss optical fibers as determined by stimulated Raman and Brillouin scattering", Applied Optics 11:2489-2494, November 1972.

3. Bielawski, W. B., "Low-loss optical waveguides: current status", Electro-optical Sys. Design 5:22-28, April 1973.

4. "Expect 2 dB/km losses in optical fibers", Electro-optical Sys. Design 5:6, July 1973.

5. Maurer, R. D.,"Glass fibers for optical communications", IEEE Proc. 61:452-462, April 1973.

6. Pearson, A. D. and French, W. G., "Low-loss glass fibers for optical transmission", Bell Lab. Record 50:103-109, April 1972.

7. Koizumi, K., et al.,"New light-focusing glass fibers made by a continuous process", 1973 IEEE/OSA Conference on Laser Engineering and Applications.

8. Chown, M. and Kao, K. C.,"Wide-band fiber waveguide communication systems for optical freguencies", Elec. Communication 46:118-124, 1971.

9. Kapron, F. P., Maurer, R. D., and Teter, M. P.,"Theory of backscattering effects in waveguides", Applied Optics 11:1352-1356, June 1972.

10. Marcuse, D., "pulse propagation in multimode dielectric waveguides", Bell Sys. Tech. Jour. 51:1199-1232, July-August 1972.

11. Gloge, D. and Marcatili, E. A. J., "Impulse response of fibers with ring-shaped parabolic index distribution", Bell Sys. Tech. Jour. 52:1161-1168, September 1973.

12. Stepke, E. T., "Optical data links: a coming attraction", Electro-optical Sys. Design 5:28-30, September 1973.

13. Sigel, G., "Radiation damage in fiber optics", DoD/Industry-Wide Integrated Optics and Fiber Optics Communications Conference, 15 May 1974.

14. Lebduska, R., "Fiber optic cable test evaluation", DoD/Industry-Wide Integrated Optics and Fiber Optics Communications Conference, 15 May 1974.

15. Stepke, E. T., "Integrating optics: Putting the pieces together", Electro-optical Sys. Design 5:18-23, September 1973.

16. Taylor, H. F., "Transfer of information on naval vessels via fiber optics transmission lines", NELC Tech. Rep. TR1763 1:52, January 1972.

17. Stigliani, J., et al., "High speed optical data links", IBM Tech. Rep. 72-531-001:76, March 1972.

INITIAL DISTRIBUTION LIST

		NO. OF COPIES
1.	Defense Documentation Center Cameron Station Alexandria, Virginia 22314	12
2.	Library, Code 0212 Naval Postgraduate School Monterey, CA 93940	2
3.	Dr. Stephen Jauregui, Jr., Code 52Ja Associate Professor of Electronics Department of Electrical Engineering Naval Postgraduate School Monterey, CA 93940	10
4.	LTjg Jessie C. Ross, USN CINCPACFLT Box 50 FPO San Francisco 96610	1
5.	Commander Naval Security Group Command 3801 Nebraska Avenue, N. W. Washington, D. C. 20390 ATTN: G80 - CDR H. Orejuela	2
6.	Naval Electronics Systems Command Naval Electronics Systems Command Headquarters Washington, D. C. 20360 ATTN: PME 107 - LCDR R. Shields	5
7.	Director National Security Agency Fort Meade, Maryland 20755 ATTN: W. Group - J. Boone	1
8.	Professor John P. Powers, Code 52Po Department of Electrical Engineering Naval Postgraduate School Monterey, CA 93940	1
9.	Naval Electronics Laboratory Center 271 Catalina Blvd San Diego, CA 92152 ATTN: Dr. Albares	1
10.	Dean of Research Naval Postgraduate School Monterey, California 93940 Attn: Code 023	1